SUPPORTING INFORMATION

Comparison of isomeric *meta*- and *para*-diiodotetrafluorobenzene as halogen bond donors in crystal engineering

Nikola Bedeković[1], *Vladimir Stilinović*[*1], *Tomislav Friščić*[2], *Dominik Cinčić*[*1]

[1]Department of Chemistry, Faculty of Science, University of Zagreb, Horvatovac 102a Zagreb, Croatia.

[2]Department of Chemistry, McGill University, 801 Sherbrooke St. W., Montreal, Canada.

E-mail: dominik@chem.pmf.hr, vstilinovic@chem.pmf.hr

Contents

Table 1. Crystallographic data of the prepared compounds.

	(**I**)(1,3-tfib)	(**II**)(1,3-tfib)	(**III**)$_2$(1,3-tfib)	(**IV**)(1,3-tfib)
Chemical formula	$C_{13}H_9NF_4I_2$	$C_{14}H_{11}NF_4I_2$	$C_{24}H_{14}N_2F_4I_2$	$C_{15}H_7NF_4I_2$
M / g mol^{-1}	509.0	523.1	660.2	531.0
Crystal system	triclinic	triclinic	monoclinic	monoclinic
Space group	$P\bar{1}$	$P\bar{1}$	$P2_1/n$	$P2_1/c$
a / Å	8.9694(9)	8.0923(12)	7.2590(50)	13.1009(14)
b/ Å	9.0988(7)	8.9366(11)	27.6970(50)	9.2198(6)
c/ Å	9.4933(12)	12.1864(22)	11.2750(50)	14.0936(14)
α	86.132(8)	94.666(13)	90	90
β	83.927(10)	92.374(14)	90.783(5)	110.087(12)
γ	81.238(7)	113.149(13)	90	90
V / Å^3	760.38(12)	805.05(4)	2266.66(19)	1598.78(75)
Z	2	2	4	4
T / K	295	295	295	295
ρ_{calc} / g cm^{-3}	2.22	2.16	1.93	2.21
μ (Mo-K_α) / mm^{-1}	4.167	3.938	2.822	3.969
$\theta_{min,max}$	$4.0 \le \theta \le 25.0$	$4.0 \le \theta \le 25.0$	$3.9 \le \theta \le 25.0$	$4.0 \le \theta \le 25.0$
$h_{min,\ max}$	$-9 \le h \le 10$	$-9 \le h \le 9$	$-8 \le h \le 8$	$-15 \le h \le 12$
$k_{min,\ max}$	$-10 \le h \le 10$	$-10 \le h \le 10$	$-32 \le k \le 24$	$-10 \le h \le 10$
$l_{min,\ max}$	$-10 \le h \le 11$	$-13 \le h \le 13$	$-13 \le l \le 13$	$-15 \le h \le 16$
F(000)	472.0	488.0	1256.0	984.0
No. meas.	5714	5757	16638	7589
No. uniq.	2638	2788	3977	2788
No. obs.	2163	1508	1411	1633
R_{int}	0.030	0.068	0.108	0.045
No. param.	184	193	289	199
$R[F^2 > 2\sigma F^2]$	0.033	0.056	0.035	0.036
$wR(F^2)$	0.089	0.138	0.605	0.072
S	1.084	0.834	0.669	0.812
$\Delta\rho_{max}$ / e Å^{-3}	0.883	1.131	0.433	0.484
$\Delta\rho_{min}$ / e Å^{-3}	−0.803	−1.297	−0.341	−0.908

Table 1. Continuation.

	(**V**)(1,3-tfib)	(**VI**)$_2$(**VI**)(1,3-tfib)	(**VII**)(**1,3-tfib**)	(**IX**)(**1,3-tfib**)
Chemical formula	$C_{19}H_9NF_4I_2$	$C_{21}H_{12}N_3F_4I_2$	$C_{10}H_4N_2F_4I_2$	$C_{10}H_9NOF_4I_2$
M / g mol^{-1}	581.1	471.2	482.0	488.0
Crystal system	monoclinic	monoclinic	monoclinic	monoclinic
Space group	$P2_1/n$	$P2_1/m$	$P2_1/c$	$P2_1/m$
a / Å	11.1020(50)	7.0063(4)	4.3271(3)	9.3023(7)
b/ Å	9.8390(50)	27.1389(17)	24.8960(17)	7.2775(5)
c/ Å	17.1180(50)	9.3619(6)	11.8038(110)	20.5704(18)
α	90	90	90	90
β	107.704(5)	98.440(5)	97.033(7)	96.422(8)
γ	90	90	90	90
V / Å^3	1781.29(33)	1760.82(13)	1262.03(11)	1383.83(13)
Z	4	4	4	4
T / K	295	295	295	295
ρ_{calc} / g cm^{-3}	2.17	1.78	2.54	2.35
μ (Mo-K_α) / mm^{-1}	3.573	1.849	5.015	4.578
$\theta_{\mu\nu,\mu\alpha\xi}$	$3.9 \le \theta \le 25.0$	$3.9 \le \theta \le 25.0$	$3.8 \le \theta \le 27.0$	$4.2 \le \theta \le 25.0$
$h_{min,\ max}$	$-13 \le h \le 12$	$-8 \le h \le 8$	$-5 \le h \le 5$	$-11 \le h \le 9$
$k_{min,\ max}$	$-11 \le h \le 11$	$-31 \le k \le 28$	$-29 \le h \le 28$	$-8 \le k \le 5$
$l_{min,\ max}$	$-20 \le h \le 19$	$-11 \le l \le 10$	$-13 \le h \le 14$	$-20 \le l \le 24$
F(000)	1088.0	920	880.0	904.0
No. meas.	8256	7351	5606	5680
No. uniq.	3108	3141	2204	2614
No. obs.	2348	2390	1841	1665
R_{int}	0.024	0.038	0.137	0.111
No. param.	235	251	163	210
$R[F^2 > 2\sigma F^2]$	0.026	0.028	0.069	0.050
$wR(F^2)$	0.053	0.062	0.181	0.150
S	0.952	0.885	1.069	0.777
$\Delta\rho_{max}$ / e Å^{-3}	0.503	0.339	2.819	0.835
$\Delta\rho_{min}$ / e Å^{-3}	−0.592	−0.802	−3.366	−0.926

Table 1. Continuation.

	(X)(1,3-tfib)	**(XI)(1,3-tfib)**	**(XII)(1,3-tfib)**	**(I)(1,4-tfib)**
Chemical formula	$C_{10}H_{10}N_2F_4I_2$	$C_{12}H_{12}N_2F_4I_2$	$C_{14}H_6N_2F_4I_2$	$C_{20}H_{18}N_2F_4I_2$
M / g mol^{-1}	487.9	514.0	532.0	616.02
Crystal system	triclinic	orthorhombic	orthorhombic	triclinic
Space group	$P\bar{1}$	$P2_1ca$	$Pn2_1a$	$P\bar{1}$
a / Å	6.1088(3)	26.5686(17)	15.1562(8)	8.2478(7)
b/ Å	9.4013(6)	9.8339(6)	7.1136(3)	8.7243(8)
c/ Å	12.4113(7)	11.9828(9)	14.3096(6)	8.9978(8)
α	103.403(5)	90	90	88.673(7)
β	96.182(4)	90	90	64.626(9)
γ	95.921(5)	90	90	66.878(8)
V / Å^3	683.21(11)	3130.78(4)	1542.79(1)	529.73(39)
Z	2	8	4	2
T / K	295	295	295	150
ρ_{calc} / g cm^{-3}	2.37	2.18	2.29	1.93
μ (Mo-K_α) / mm^{-1}	4.633	4.050	4.115	3.010
$\theta_{\mu\nu,\mu\alpha\xi}$	$4.0 \le \theta \le 25$	$4.3 \le \theta \le 25.0$	$3.9 \le \theta \le 27.0$	$4.4 \le \theta \le 25$
$h_{min,\ max}$	$-7 \le h \le 7$	$-31 \le h \le 31$	$-19 \le h \le 14$	$-9 \le h \le 8$
$k_{min,\ max}$	$-11 \le h \le 11$	$-11 \le h \le 11$	$-9 \le k \le 9$	$-9 \le h \le 10$
$l_{min,\ max}$	$-14 \le h \le 9$	$-14 \le h \le 13$	$-16 \le l \le 17$	$-10 \le h \le 10$
F(000)	452.0	1920.0	984.0	294.0
No. meas.	4637	15526	5840	3477
No. uniq.	2386	5388	2958	1799
No. obs.	1855	4355	2253	1676
R_{int}	0.036	0.077	0.091	0.019
No. param.	170	362	199	129
$R[F^2 > 2\sigma F^2]$	0.036	0.080	0.052	0.024
$wR(F^2)$	0.089	0.232	0.128	0.063
S	0.997	1.106	0.973	1.061
$\Delta\rho_{max}$ / e Å^{-3}	0.712	2.448	2.152	0.891
$\Delta\rho_{min}$ / e Å^{-3}	−1.177	−2.117	−1.407	−0.561

Table 1. Continuation

	(II)(1,4-tfib)	**(III)(1,4-tfib)**	**(IV)(1,4-tfib)**	**(VII)(1,4-tfib)**
Chemical formula	$C_{14}H_{11}NF_4I_2$	$C_{24}H_{14}N_2F_4I_2$	$C_{24}H_{14}N_2F_4I_2$	$C_{10}H_4N_2I_2F_4$
M / g mol^{-1}	523.1	660.04	660.04	482.0
Crystal system	monoclinic	monoclinic	monoclinic	Triclinic
Space group	*C*2/*c*	$P2_1/n$	$P2_1/n$	*P*−1
a / Å	7.4488(0)	4.2847(4)	8.7924(11)	5.7902(3)
b/ Å	17.9710(29)	11.5355(13)	6.0635(9)	8.7132(5)
c/ Å	12.0470(15)	22.4615(17)	21.7032(21)	13.4792(7)
α	90	90	90	72.603(5)
β	93.771(23)	93.759(7)	100.650(11)	79.867(4)
γ	90	90	90	85.571(4)
V / Å^3	1609.13(25)	1107.80(5)	1137.13(24)	638.59(11)
Z	4	4	4	2
T / K	150	150	150	295
ρ_{calc} / g cm^{-3}	2.16	1.98	1.93	2.51
μ (Mo-K_α) / mm^{-1}	3.941	2.887	2.812	4.955
$\theta_{\mu\nu,\mu\alpha\xi}$	$4.1 \le \theta \le 25$	$4.0 \le \theta \le 25.0$	$4.3 \le \theta \le 25.0$	$4.4 \le \theta \le 27.0$
$h_{min,\ max}$	$-7 \le h \le 8$	$-5 \le h \le 5$	$-9 \le h \le 10$	$-6 \le h \le 7$
$k_{min,\ max}$	$-21 \le h \le 21$	$-13 \le k \le 13$	$-6 \le h \le 7$	$-11 \le h \le 11$
$l_{min,\ max}$	$-14 \le h \le 14$	$-22 \le l \le 26$	$-25 \le h \le 25$	$-16 \le h \le 17$
F(000)	976.0	628.0	628.0	440.0
No. meas.	5593	6919	5431	4030
No. uniq.	1420	1935	1985	2712
No. obs.	1182	1474	1568	2191
R_{int}	0.193	0.030	0.052	0.022
No. param.	101	145	145	164
$R[F^2 > 2\sigma F^2]$	0.048	0.024	0.045	0.026
$wR(F^2)$	0.125	0.052	0.115	0.063
S	1.010	0.963	1.160	0.936
$\Delta\rho_{max}$ / e Å^{-3}	1.603	0.415	0.972	0.628
$\Delta\rho_{min}$ / e Å^{-3}	−1.811	−0.496	−0.676	−0.816

Table 1. Continuation.

	(XII)(1,4-tfib)	**(XIII)(1,4-tfib)**	**(XIV)(1,4-tfib)**	**(XV)(1,4-tfib)**
Chemical formula	$C_{14}H_6N_2F_4I_2$	$C_{18}H_{14}N_2F_4I_2$	$C_{18}H_{14}N_2F_4I_2$	$C_{18}H_{14}N_2F_4I_2$
M / g mol^{-1}	532.0	550.0	588.11	588.11
Crystal system	monoclinic	monoclinic	monoclinic	triclinic
Space group	$P2_1/n$	$P2_1/c$	$P2_1/n$	$P\bar{1}$
a / Å	12.0566(6)	6.7235(4)(6)	11.2777(22)	6.2409(3)
b/ Å	6.1409(3)	18.3649(9)	5.5135(12)	8.4295(5)
c/ Å	21.3074(10)	8.1296(6)	15.6496(26)	9.1751(5)
α	90	90	90	80.934(5)
β	100.917(4)	107.109(7)	93.572(16)	84.467(4)
γ	90	90	90	78.592(5)
V / Å^3	1549.02(12)	959.39(22)	971.20	466.17
Z	4	4	4	2
ρ_{calc} / g cm^{-3}	2.28	2.04	2.01	2.09
μ (Mo-K_α) / mm^{-1}	4.098	3.319	3.279	3.415
$\theta_{\mu\nu,\mu\alpha\xi}$	$3.9 \leq \theta \leq 25.0$	$3.9 \leq \theta \leq 27.0$	$3.9 \leq \theta \leq 27.0$	$4.1 \leq \theta \leq 25.0$
$h_{min,\ max}$	$-14 \leq h \leq 14$	$-8 \leq h \leq 8$	$-14 \leq h \leq 14$	$-7 \leq h \leq 7$
$k_{min,\ max}$	$-7 \leq h \leq 7$	$-15 \leq k \leq 23$	$-6 \leq h \leq 7$	$-9 \leq h \leq 6$
$l_{min,\ max}$	$-25 \leq h \leq 25$	$-8 \leq l \leq 10$	$-19 \leq h \leq 19$	$-10 \leq h \leq 10$
F(000)	984.0	556.0	556.0	278.0
No. meas.	10652	5317	8829	2331
No. uniq.	2716	2067	2090	1529
No. obs.	1910	1801	1657	1397
R_{int}	0.031	0.075	0.064	0.049
No. param.	200	119	119	119
$R[F^2 > 2\sigma F^2]$	0.030	0.046	0.027	0.033
$wR(F^2)$	0.080	0.103	0.060	0.085
S	1.010	1.168	0.969	1.092
$\Delta\rho_{max}$ / e Å^{-3}	0.639	1.649	0.906	1.171
$\Delta\rho_{min}$ / e Å^{-3}	−0.644	−1.041	−0.710	−1.825

Table 2. Crystallographic unit cell volumes for equivalent structures of **1,3-tfib** ($V_{1,3}$) and **1,4-tfib** ($V_{1,4}$) cocrystals with identical halogen bond acceptors and stoichiometric compositions, corresponding unit cell volume per Z ,$(V/Z)_{1,3}$ and $(V/Z)_{1,4}$, and their relative difference Δ ($\frac{(V/Z)_{1,3} - (V/Z)_{1,4}}{(V/Z)_{1,4}}$)

acceptor	$V_{1,3}$ (Å^3)	$(V/Z)_{1,3}$ (Å^3)	$V_{1,4}$ (Å^3)	$(V/Z)_{1,4}$ (Å^3)	Δ (%)
II	805.1	402.6	1609.1	402.3	+0.08
III	2266.7	566.7	1107.8	553.9	+2.3
VII	1262.0	315.5	638.6	319.3	-1.2
VIII	850.6	425.3	842.2	421.1	+1.0
IX	1383.8	346.0	325.6	325.6	+6.3
X	683.3	341.7	324.6	324.6	+5.3
XI	3130.8	391.4	773.7	386.9	+1.2
XII	1542.8	385.7	1549.0	387.3	-0.4
XVI	2239.5	1119.8	1097.6	1097.6	+2.0

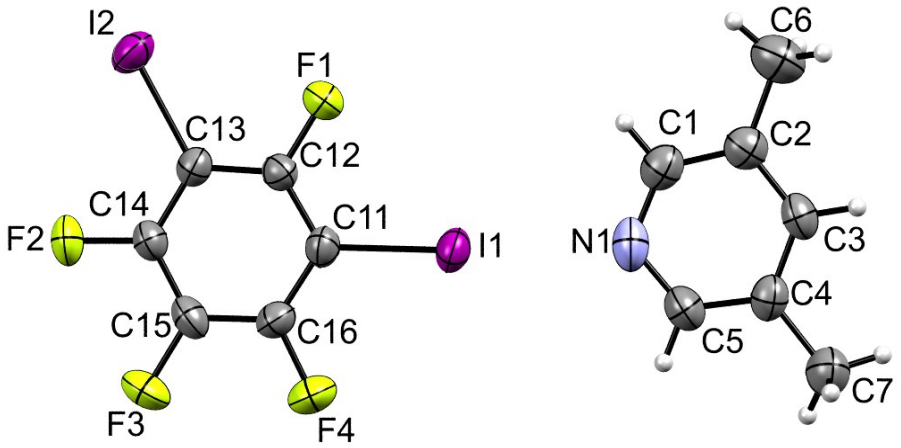

Figure 1. Molecular structure of (**I**)(**1,3-tfib**) showing the atom-labelling scheme. Displacement ellipsoids are drawn at the 50 % probability level, and H atoms are shown as small spheres of arbitrary radius.

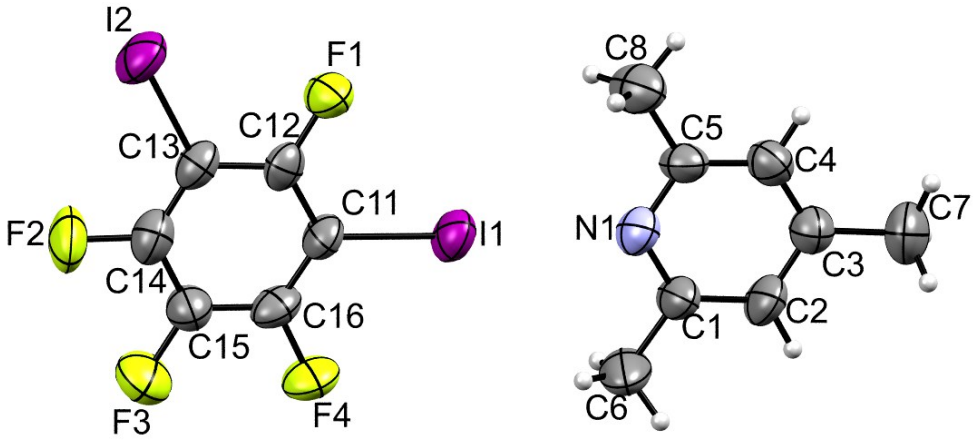

Figure 2. Molecular structure of (**II**)(**1,3-tfib**) showing the atom-labelling scheme. Displacement ellipsoids are drawn at the 50 % probability level, and H atoms are shown as small spheres of arbitrary radius.

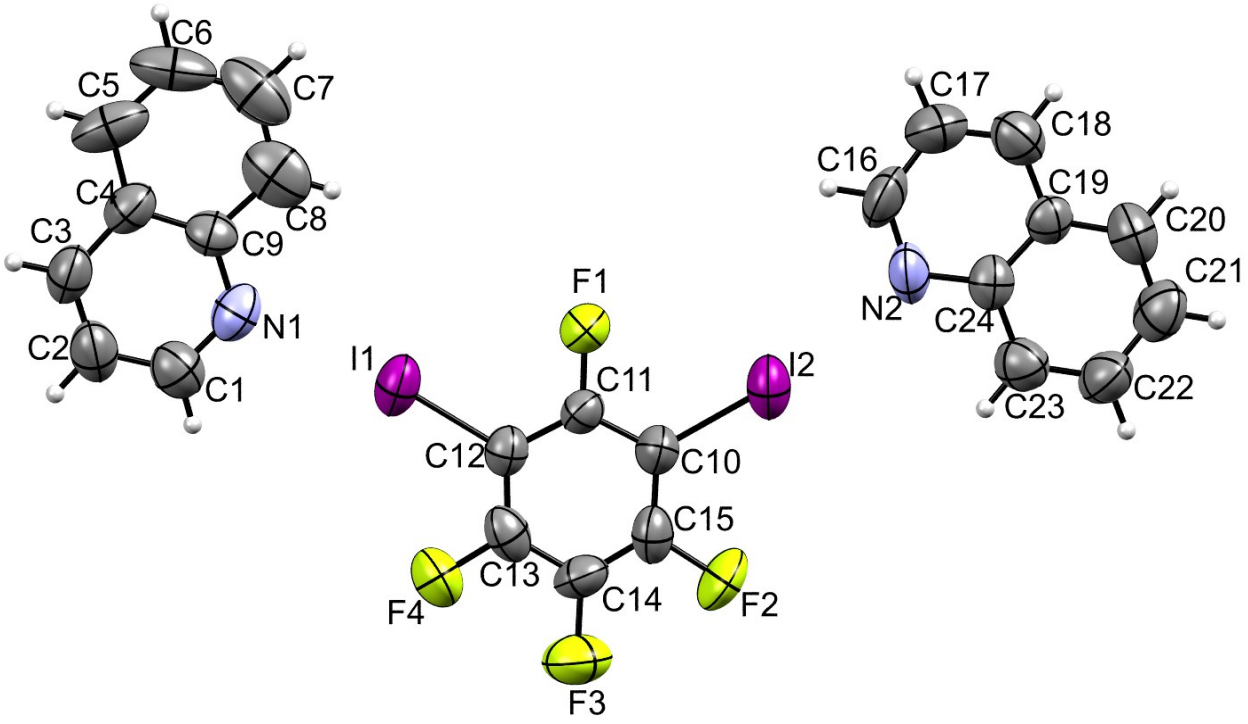

Figure 3. Molecular structure of (**III**)$_2$(**1,3-tfib**) showing the atom-labelling scheme. Displacement ellipsoids are drawn at the 50 % probability level, and H atoms are shown as small spheres of arbitrary radius.

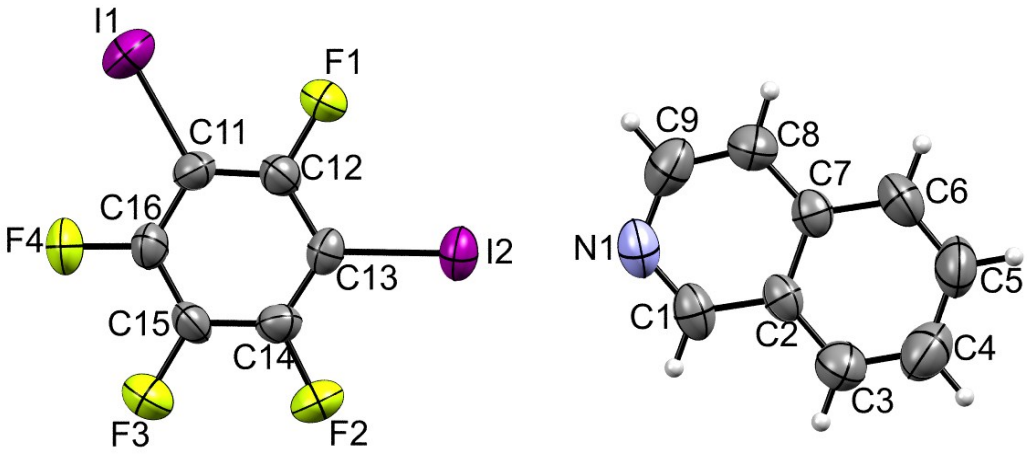

Figure 4. Molecular structure of (**IV**)(**1,3-tfib**) showing the atom-labelling scheme. Displacement ellipsoids are drawn at the 50 % probability level, and H atoms are shown as small spheres of arbitrary radius.

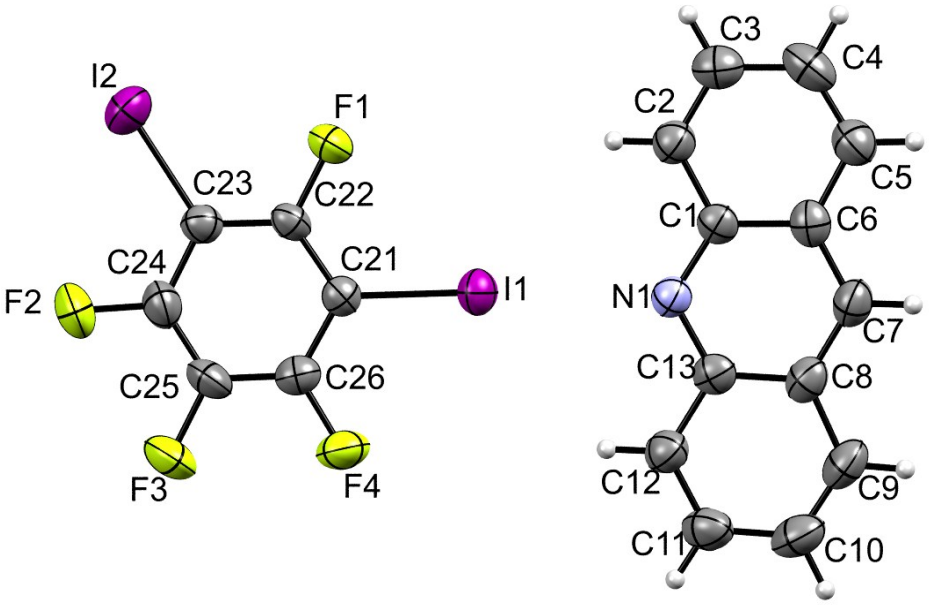

Figure 5. Molecular structure of (**V**)(**1,3-tfib**) showing the atom-labelling scheme. Displacement ellipsoids are drawn at the 50 % probability level, and H atoms are shown as small spheres of arbitrary radius.

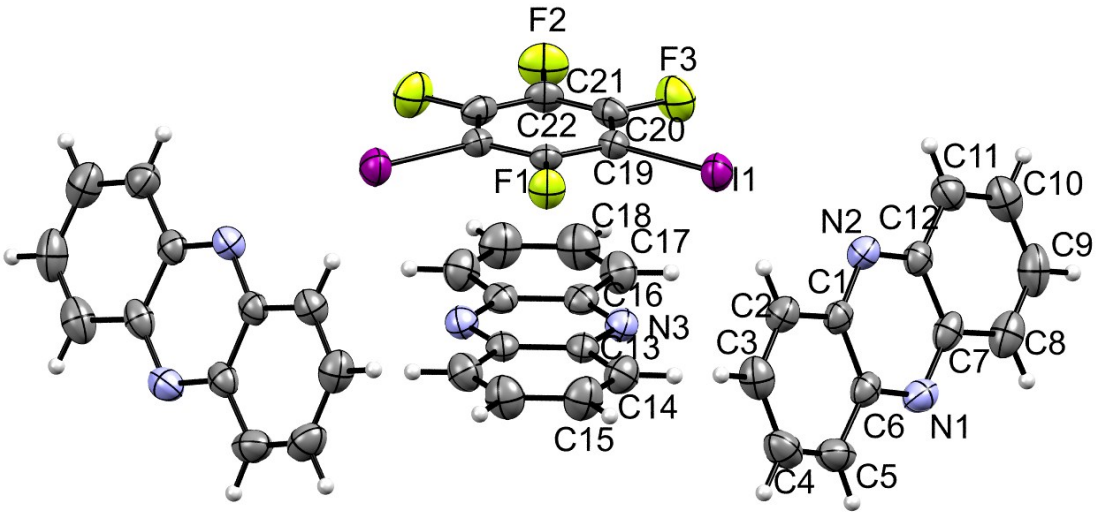

Figure 6. Molecular structure of (**VI**)$_2$(**VI**)(**1,3-tfib**) showing the atom-labelling scheme. Displacement ellipsoids are drawn at the 50 % probability level, and H atoms are shown as small spheres of arbitrary radius.

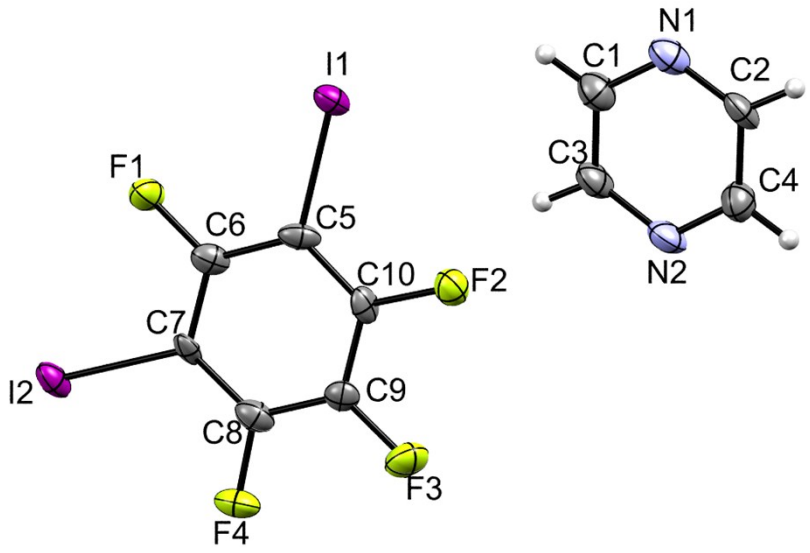

Figure 7. Molecular structure of (**VII**)(**1,3-tfib**) showing the atom-labelling scheme. Displacement ellipsoids are drawn at the 50 % probability level, and H atoms are shown as small spheres of arbitrary radius.

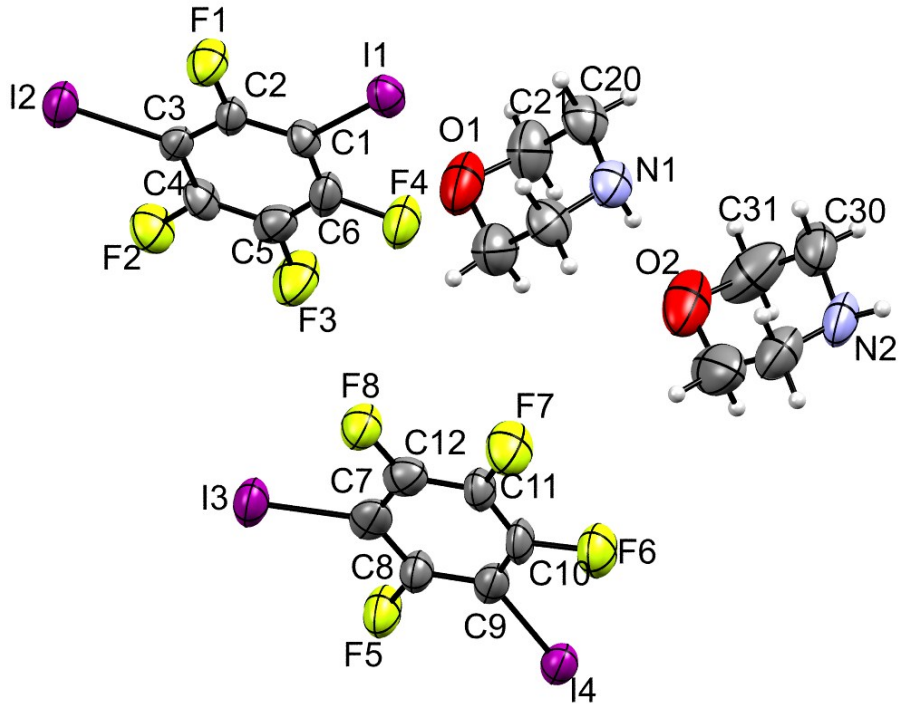

Figure 8. Molecular structure of (**IX**)(**1,3-tfib**) showing the atom-labelling scheme. Displacement ellipsoids are drawn at the 50 % probability level, and H atoms are shown as small spheres of arbitrary radius..

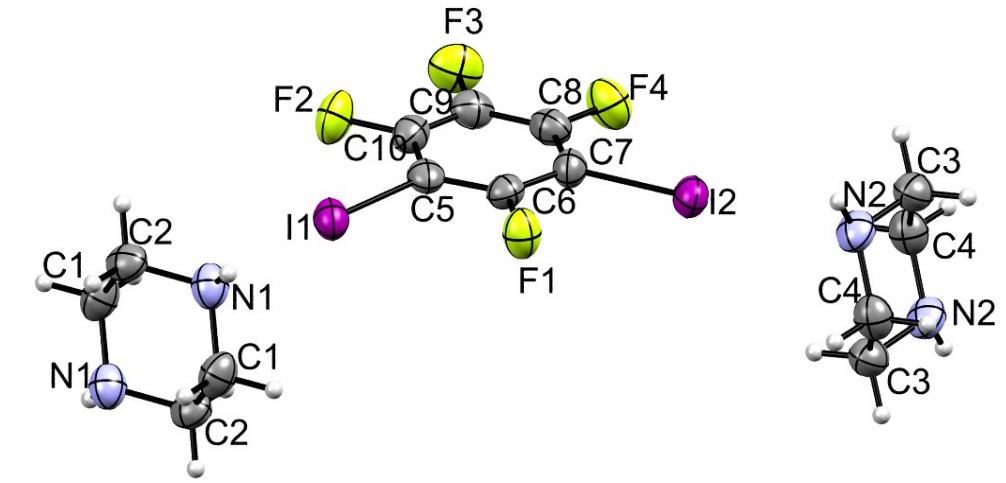

Figure 9. Molecular structure of (**X**)(**1,3-tfib**) showing the atom-labelling scheme. Displacement ellipsoids are drawn at the 50 % probability level, and H atoms are shown as small spheres of arbitrary radius.

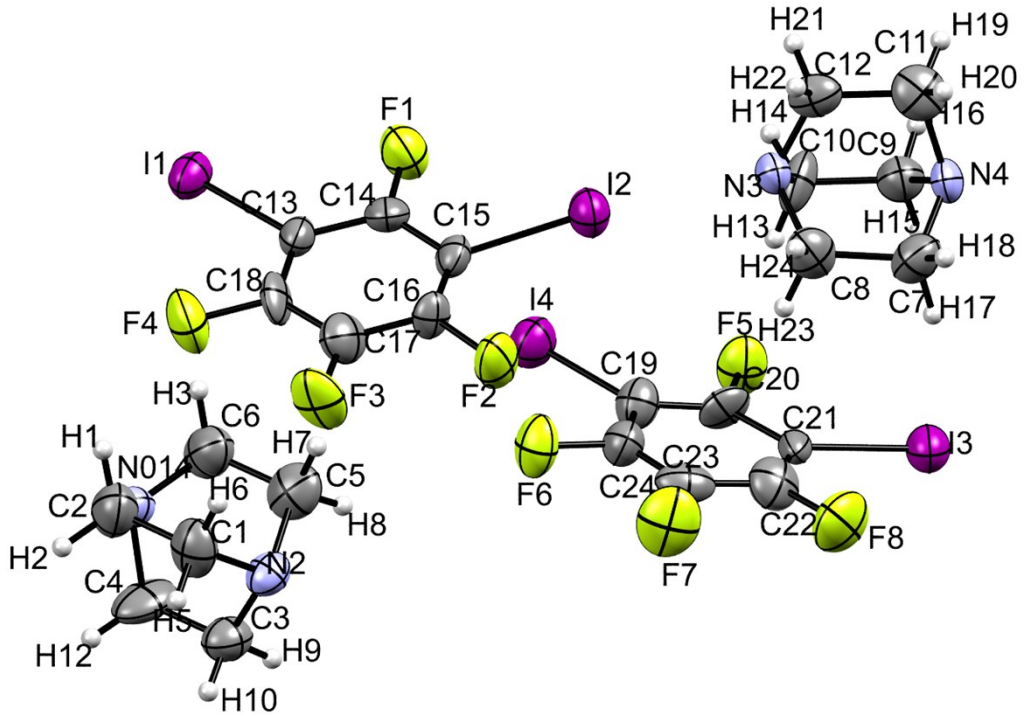

Figure 10. Molecular structure of (**XI**)(**1,3-tfib**) showing the atom-labelling scheme. Displacement ellipsoids are drawn at the 50 % probability level, and H atoms are shown as small spheres of arbitrary radius.

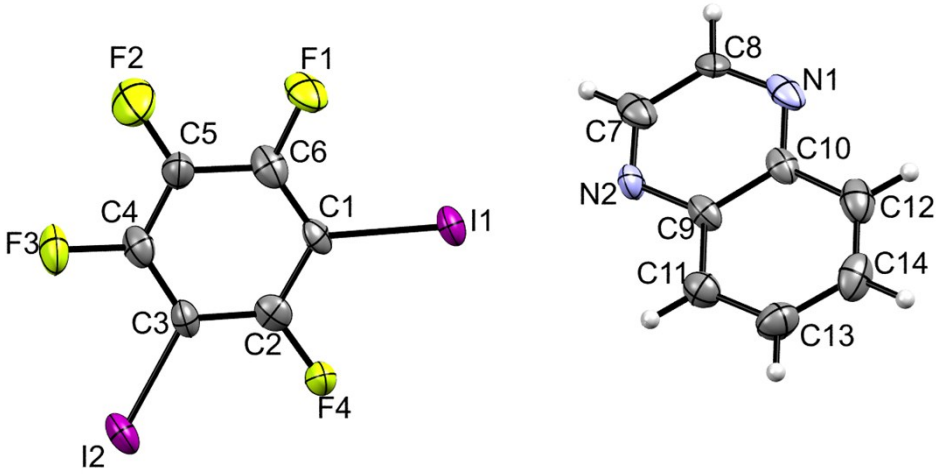

Figure 11. Molecular structure of (**XII**)(**1,3-tfib**) showing the atom-labelling scheme. Displacement ellipsoids are drawn at the 50 % probability level, and H atoms are shown as small spheres of arbitrary radius.

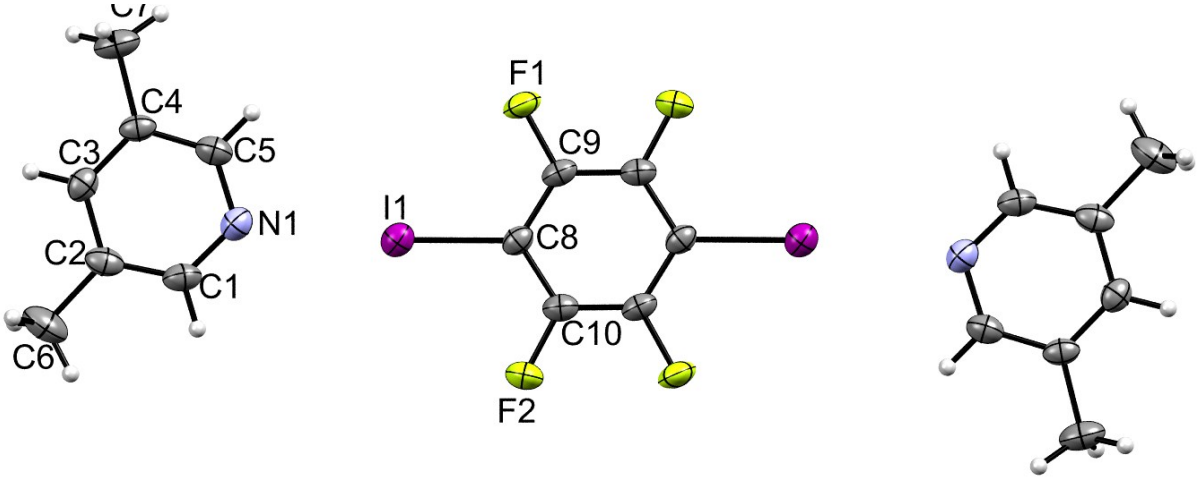

Figure 12. Molecular structure of (**I**)$_2$(**1,4-tfib**) showing the atom-labelling scheme. Displacement ellipsoids are drawn at the 50 % probability level, and H atoms are shown as small spheres of arbitrary radius.

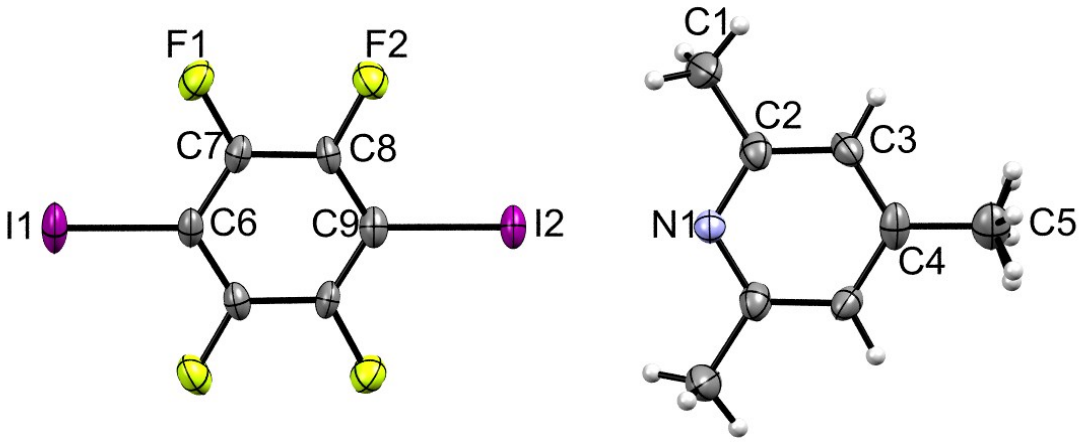

Figure 13. Molecular structure of (**II**)(**1,4-tfib**) showing the atom-labelling scheme. Displacement ellipsoids are drawn at the 50 % probability level, and H atoms are shown as small spheres of arbitrary radius.

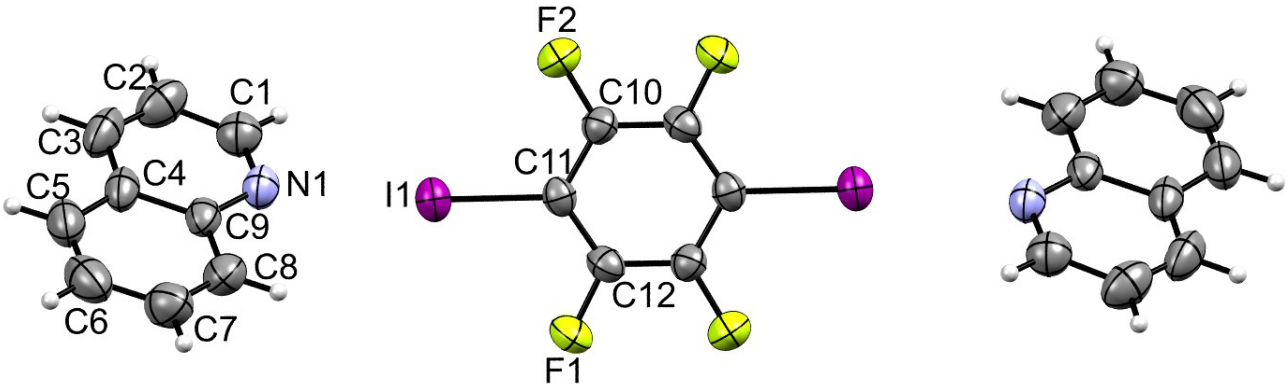

Figure 14. Molecular structure of (**III**)$_2$(**1,4-tfib**) showing the atom-labelling scheme. Displacement ellipsoids are drawn at the 50 % probability level, and H atoms are shown as small spheres of arbitrary radius.

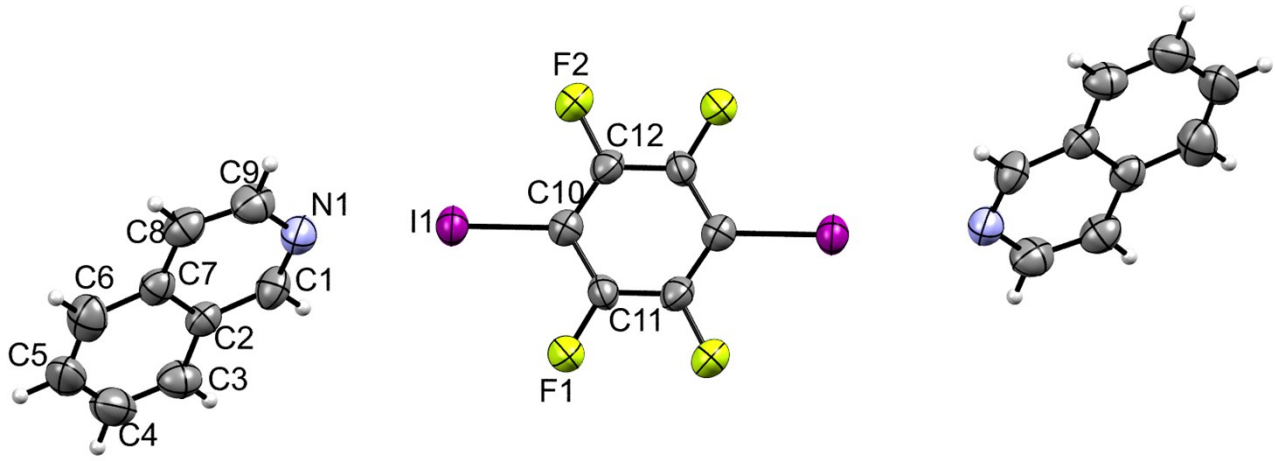

Figure 15. Molecular structure of (**IV**)$_2$(**1,4-tfib**) showing the atom-labelling scheme. Displacement ellipsoids are drawn at the 50 % probability level, and H atoms are shown as small spheres of arbitrary radius.

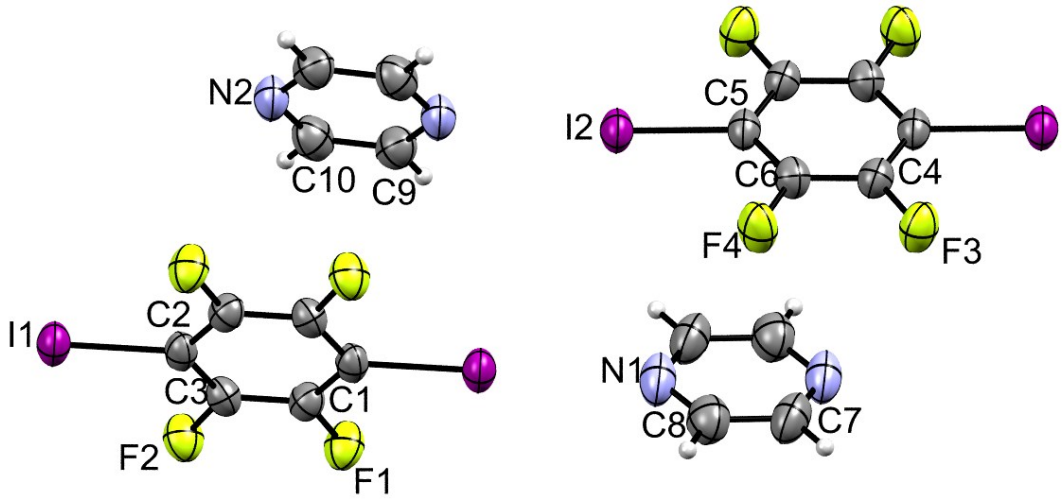

Figure 16. Molecular structure of (**VII**)(**1,4-tfib**) showing the atom-labelling scheme. Displacement ellipsoids are drawn at the 50 % probability level, and H atoms are shown as small spheres of arbitrary radius.

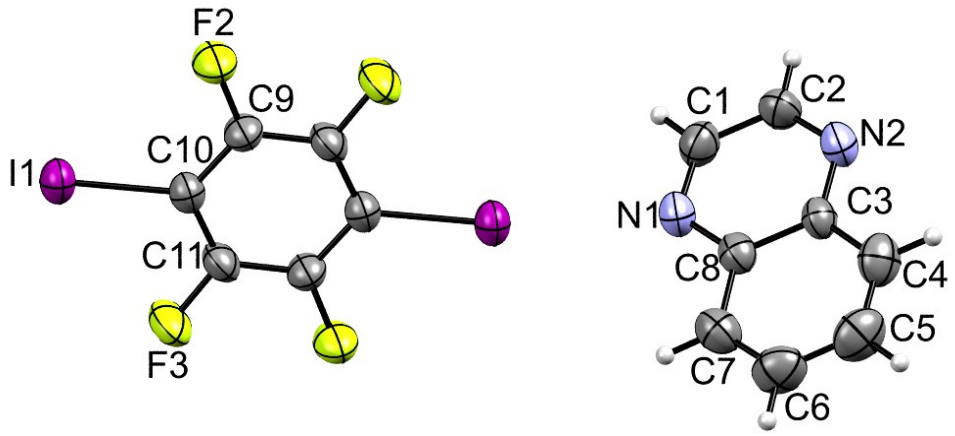

Figure 17. Molecular structure of (**XII**)(**1,4-tfib**) showing the atom-labelling scheme. Displacement ellipsoids are drawn at the 50 % probability level, and H atoms are shown as small spheres of arbitrary radius.

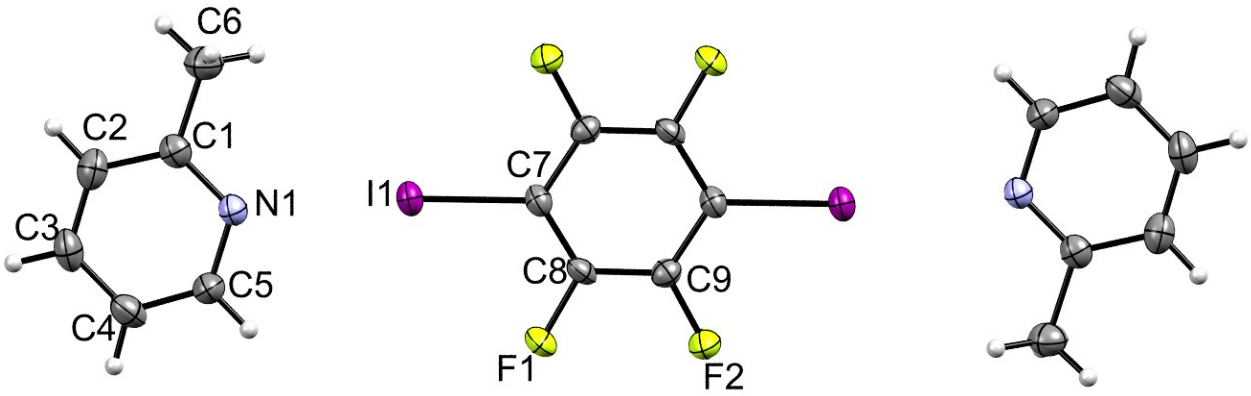

Figure 18. Molecular structure of (**XIII**)$_2$(**1,4-tfib**) showing the atom-labelling scheme. Displacement ellipsoids are drawn at the 50 % probability level, and H atoms are shown as small spheres of arbitrary radius.

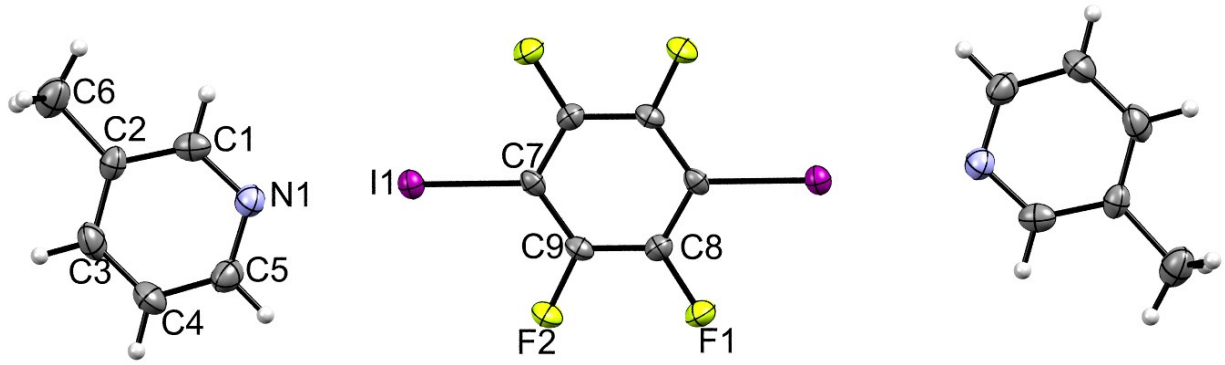

Figure 19. Molecular structure of (**XIV**)$_2$(**1,4-tfib**) showing the atom-labelling scheme. Displacement ellipsoids are drawn at the 50 % probability level, and H atoms are shown as small spheres of arbitrary radius.

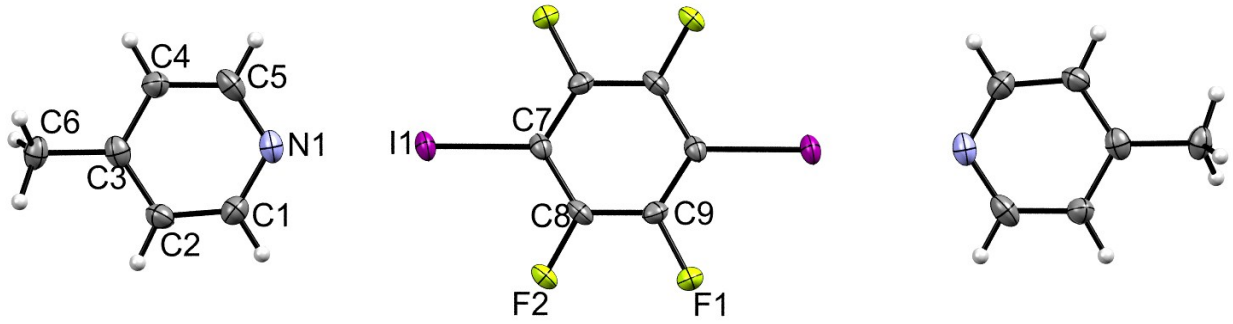

Figure 20. Molecular structure of (**XV**)$_2$(**1,4-tfib**) showing the atom-labelling scheme. Displacement ellipsoids are drawn at the 50 % probability level, and H atoms are shown as small spheres of arbitrary radius.

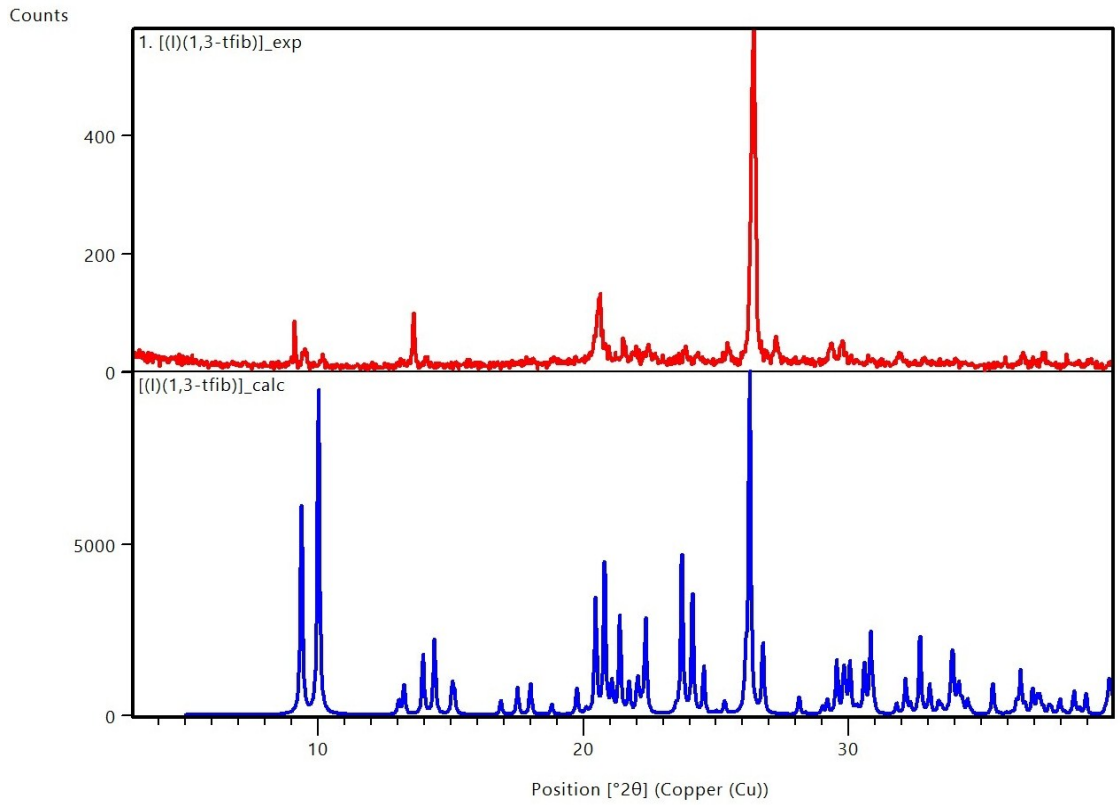

Figure 21. Experimental and calculated XRPD patterns of the (**I**)(**1,3-tfib**).

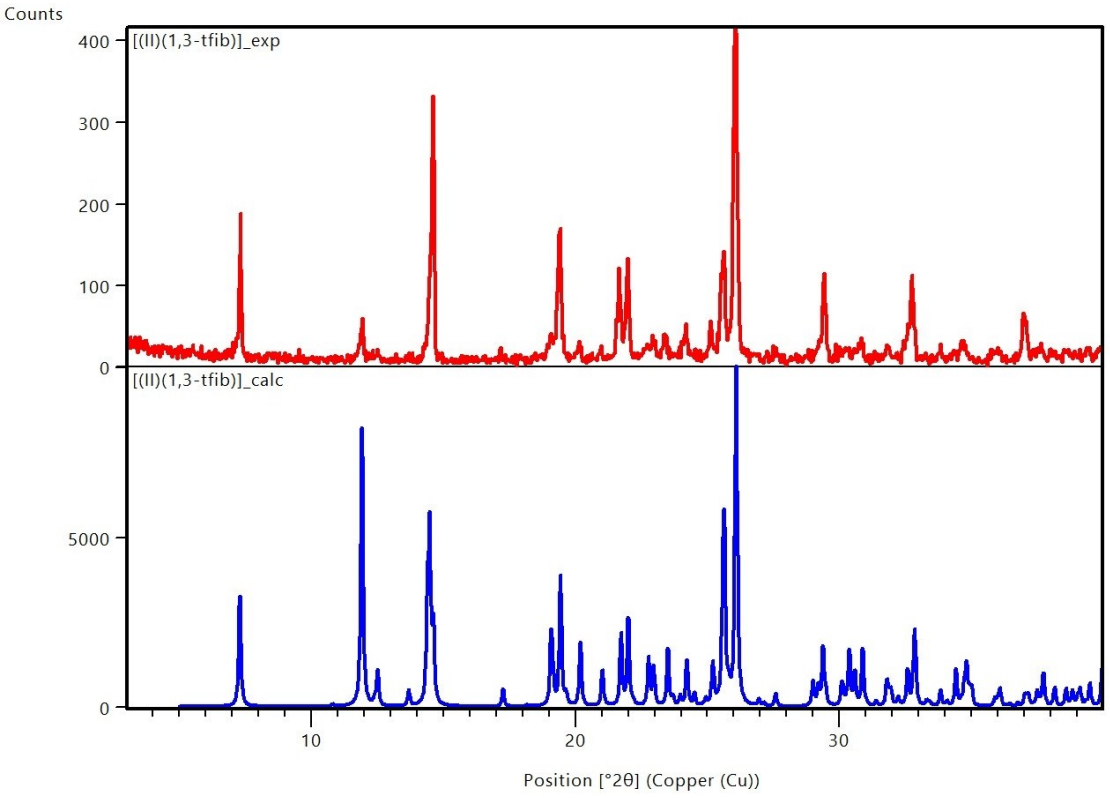

Figure 22. Experimental and calculated XRPD patterns of the (**II**)(**1,3-tfib**).

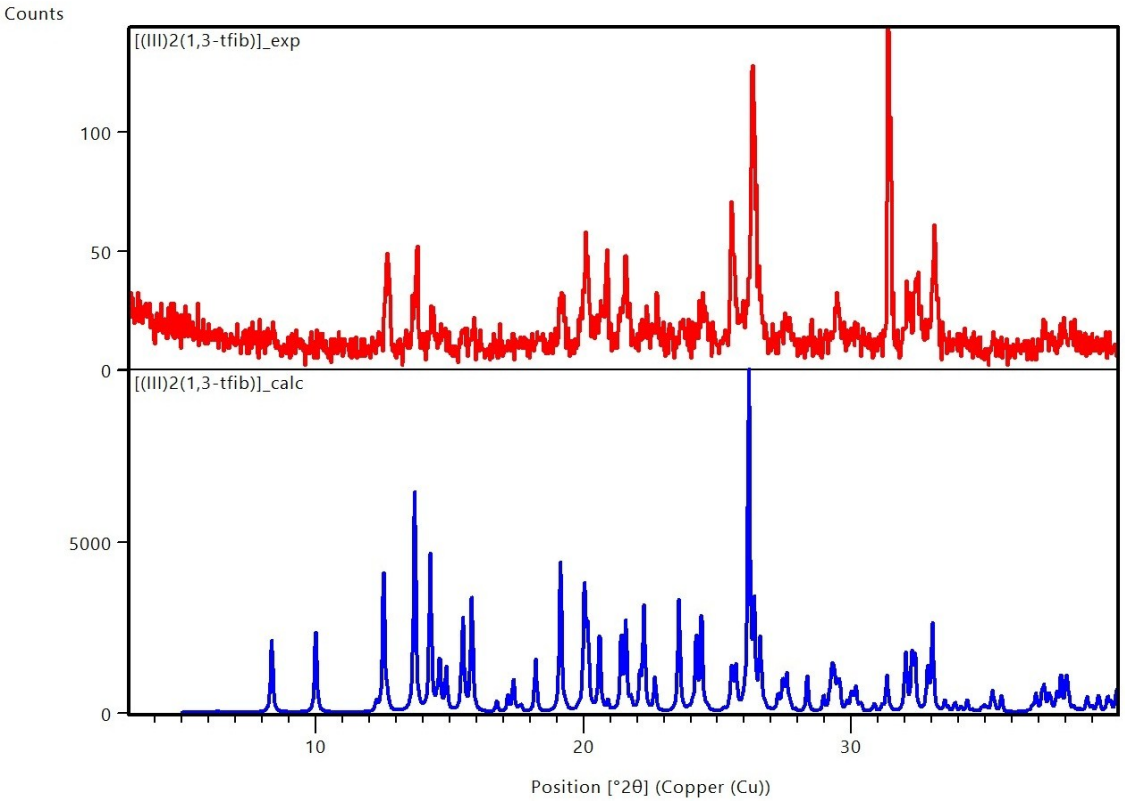

Figure 23. Experimental and calculated XRPD patterns of the (**III**)$_2$(**1,3-tfib**).

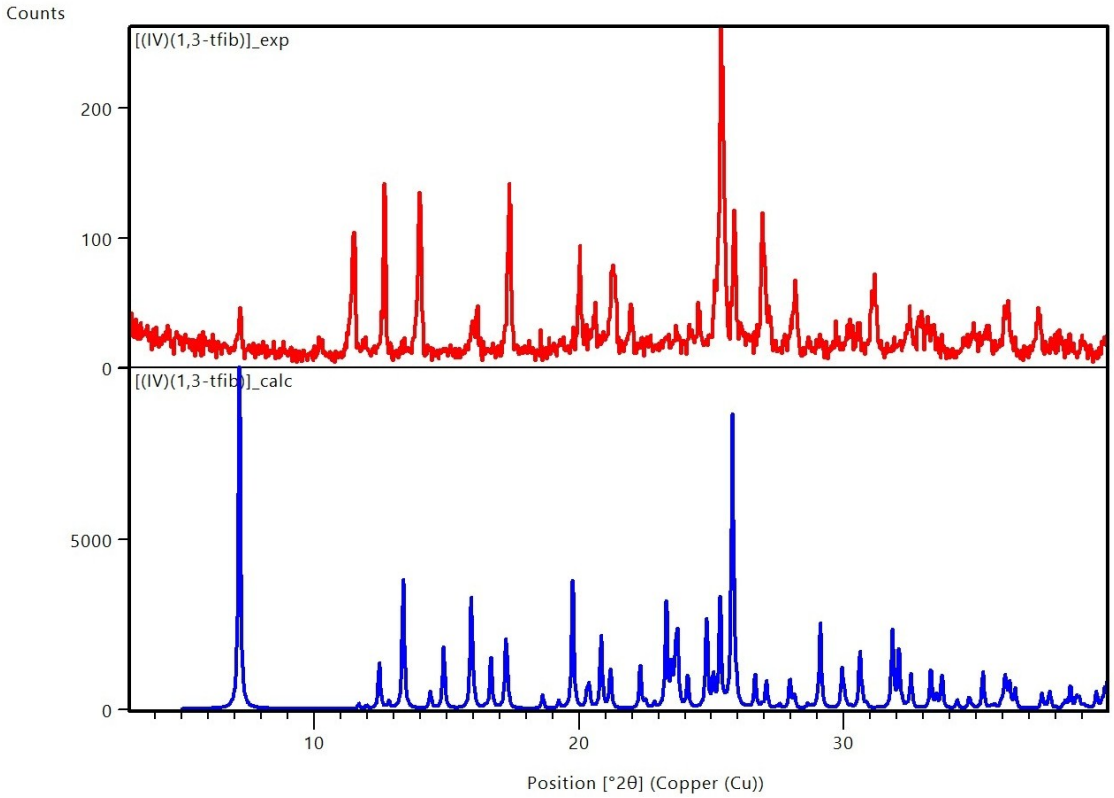

Figure 24. Experimental and calculated XRPD patterns of the (**IV**)(**1,3-tfib**).

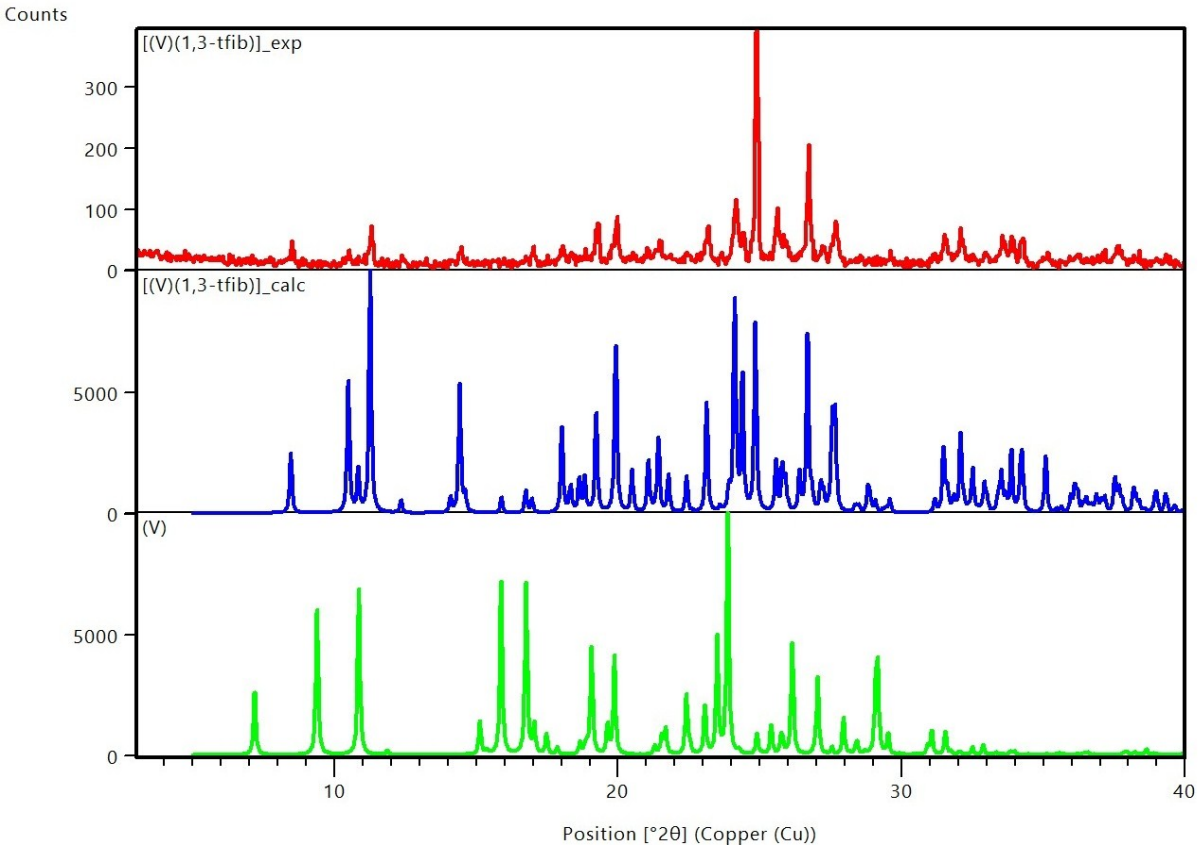

Figure 25. Experimental and calculated XRPD patterns of the (**V**)(**1,3-tfib**) and **V**.

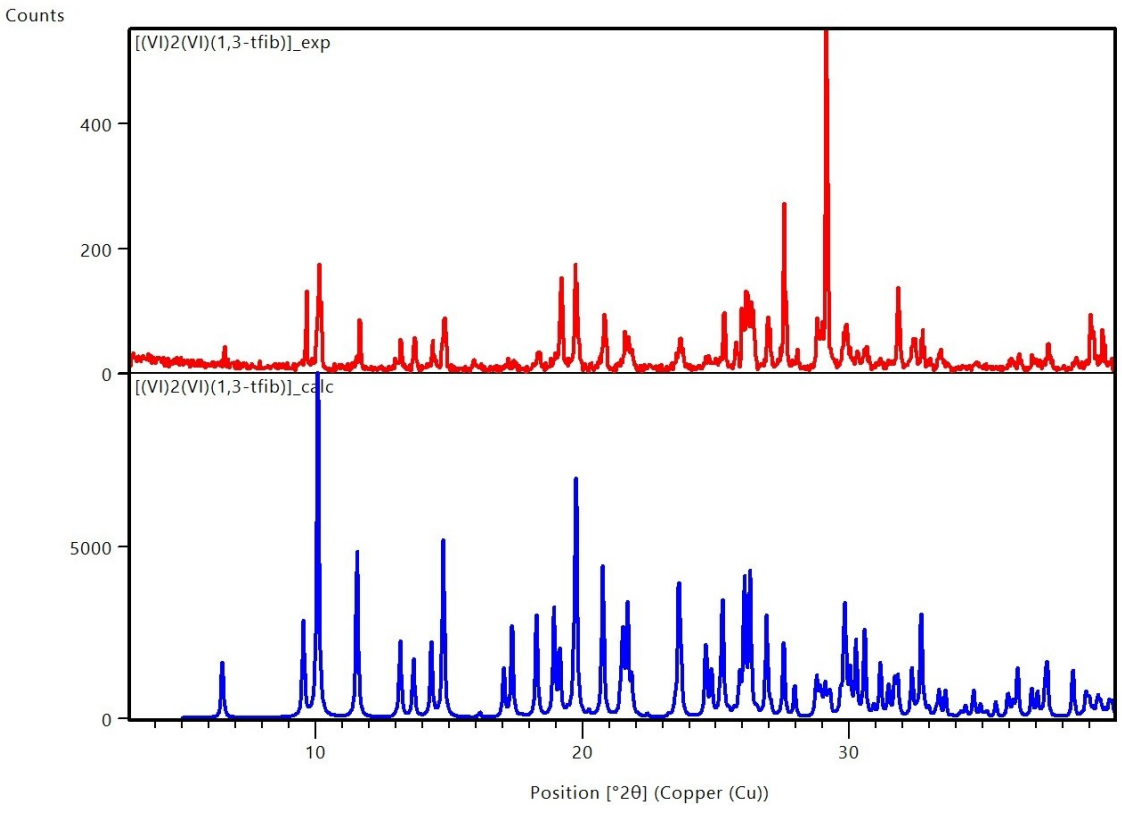

Figure 26. Experimental and calculated XRPD patterns of the (**VI**)$_2$(**VI**)(**1,3-tfib**).

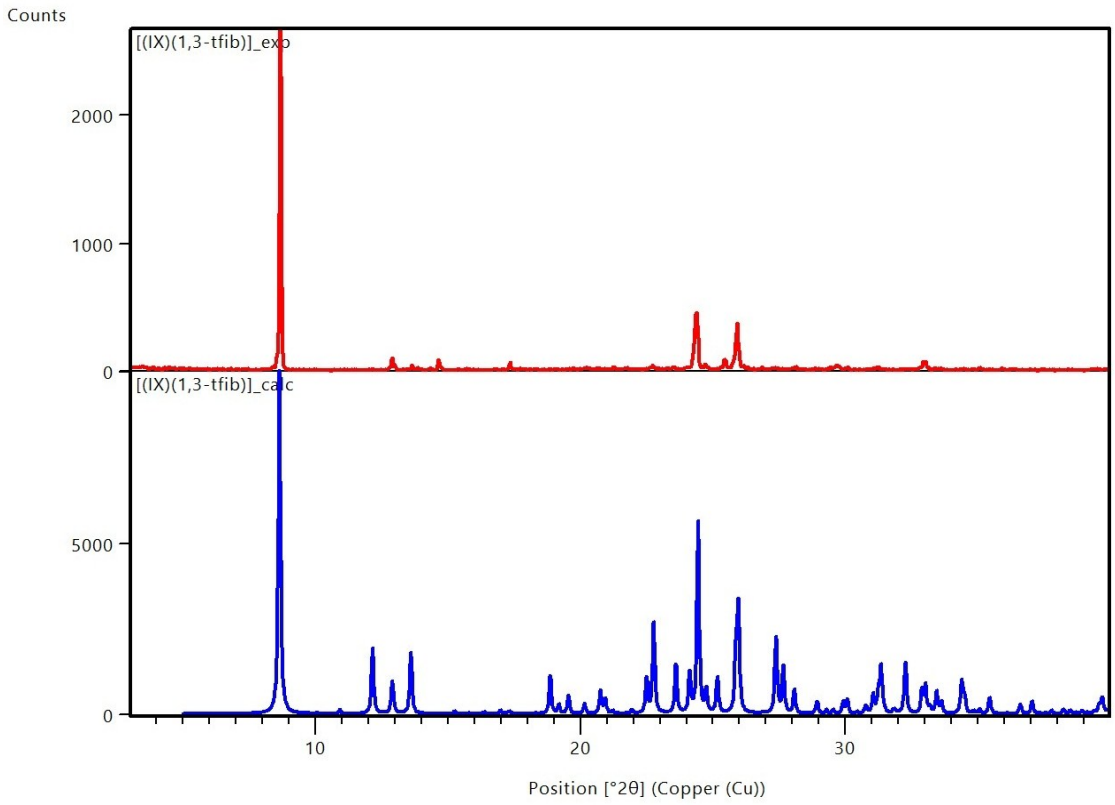

Figure 27. Experimental and calculated XRPD patterns of the (**IX**)(**1,3-tfib**).

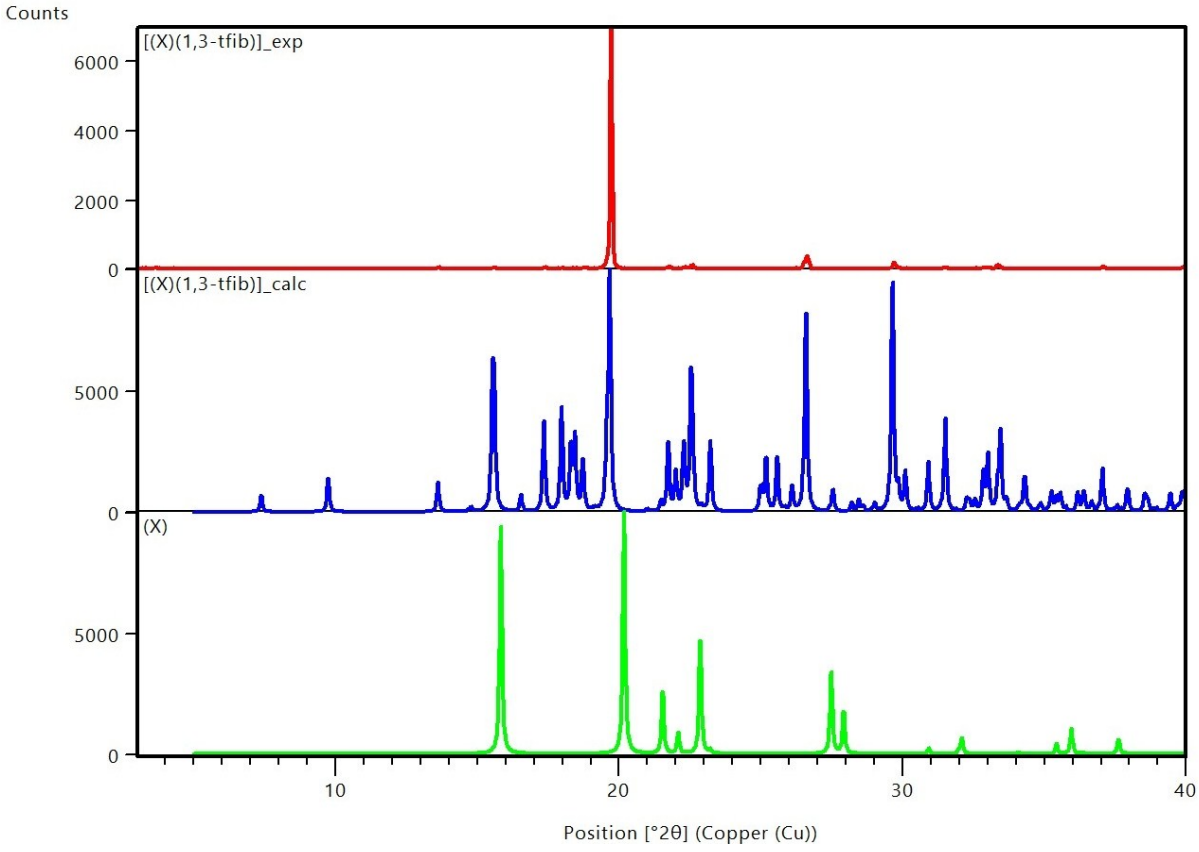

Figure 28. Experimental and calculated XRPD patterns of the (**X**)(**1,3-tfib**) and X.

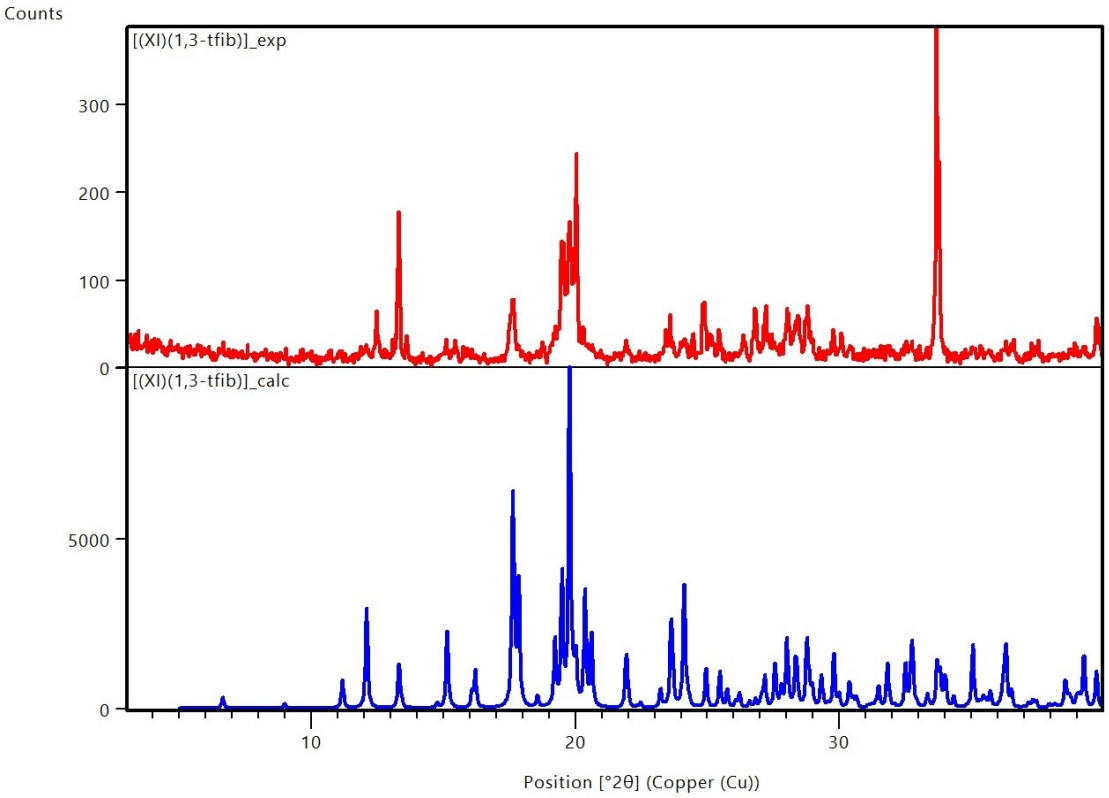

Figure 29. Experimental and calculated XRPD patterns of the (**XI**)(**1,3-tfib**).

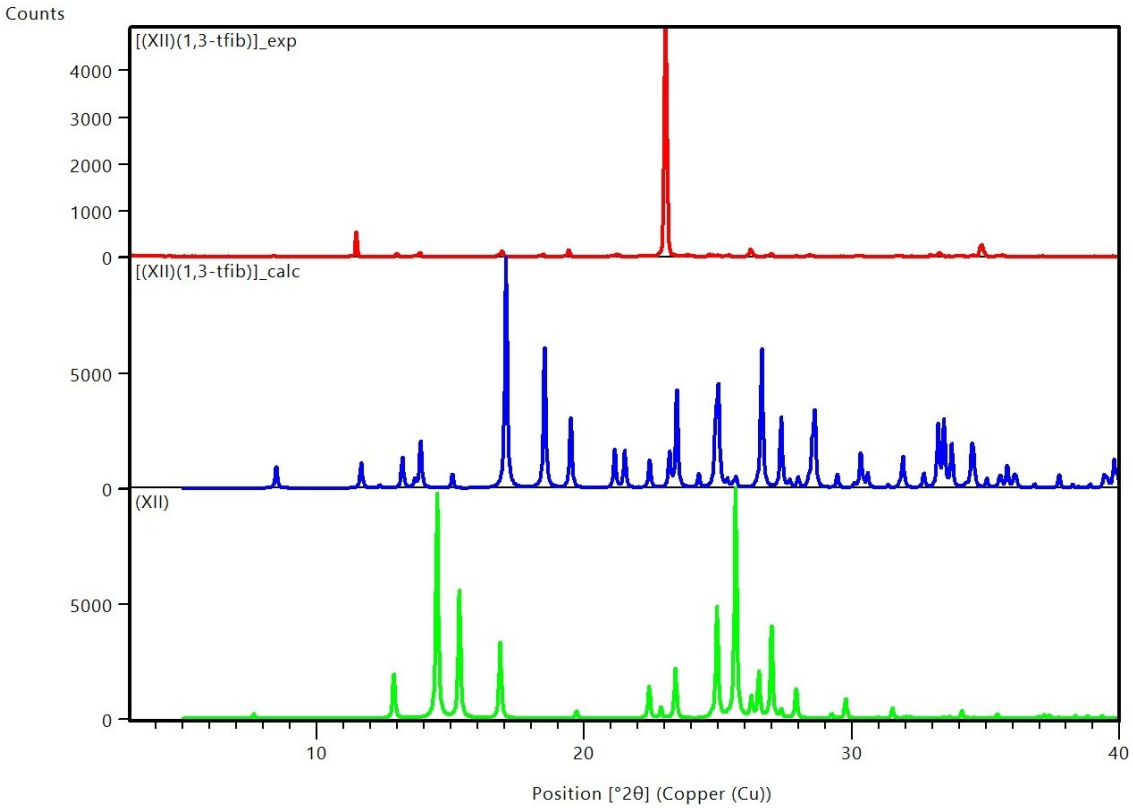

Figure 30. Experimental and calculated XRPD patterns of the (**XII**)(**1,3-tfib**) and XII.

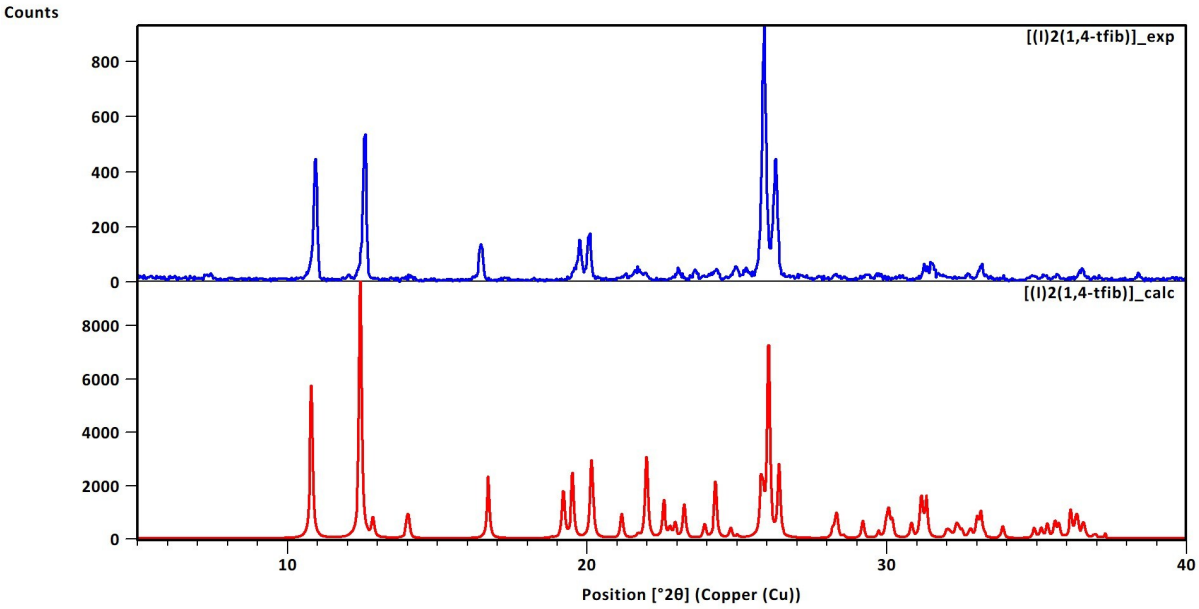

Figure 31. Experimental and calculated XRPD patterns of the (**I**)$_2$(**1,4-tfib**).

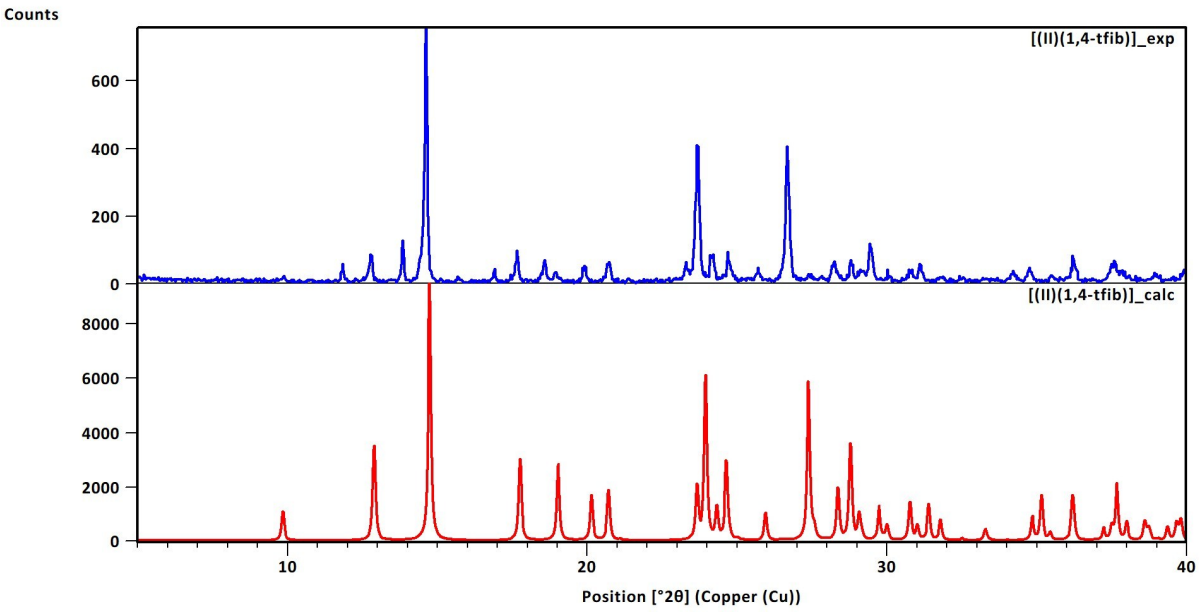

Figure 32. Experimental and calculated XRPD patterns of the (**II**)(**1,4-tfib**).

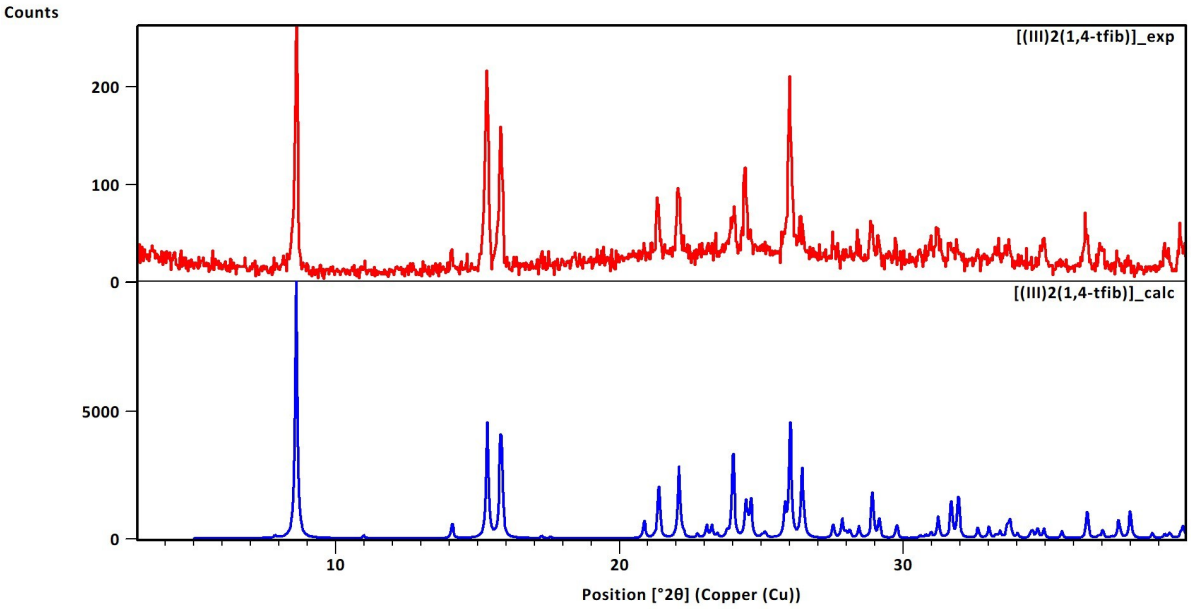

Figure 33. Experimental and calculated XRPD patterns of the (**III**)$_2$(**1,4-tfib**).

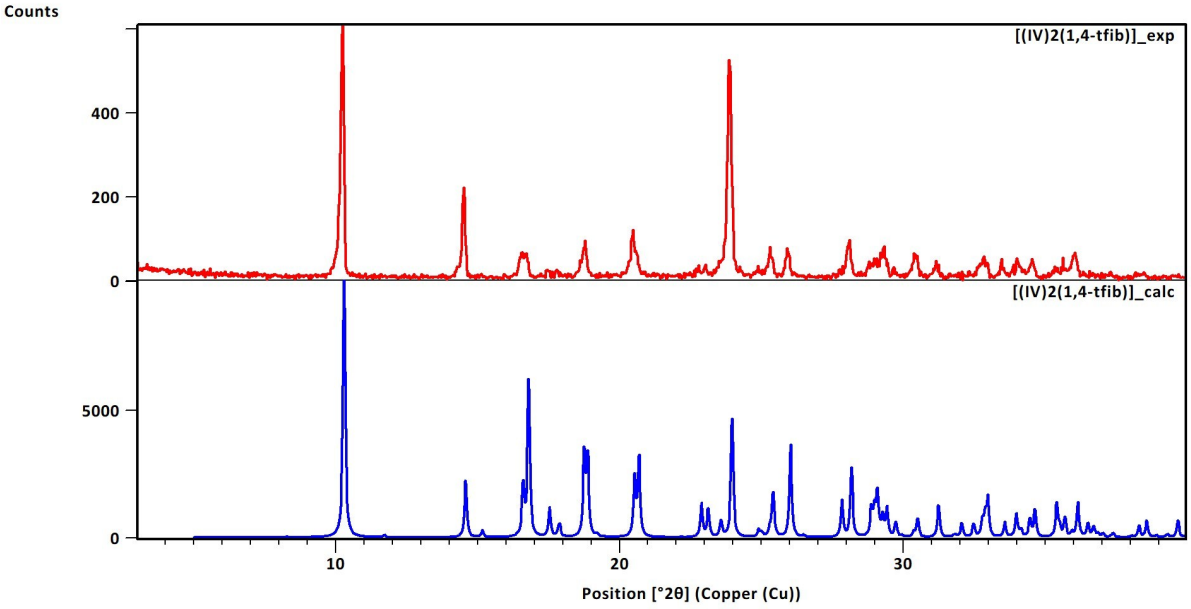

Figure 34. Experimental and calculated XRPD patterns of the (**IV**)$_2$(**1,4-tfib**).

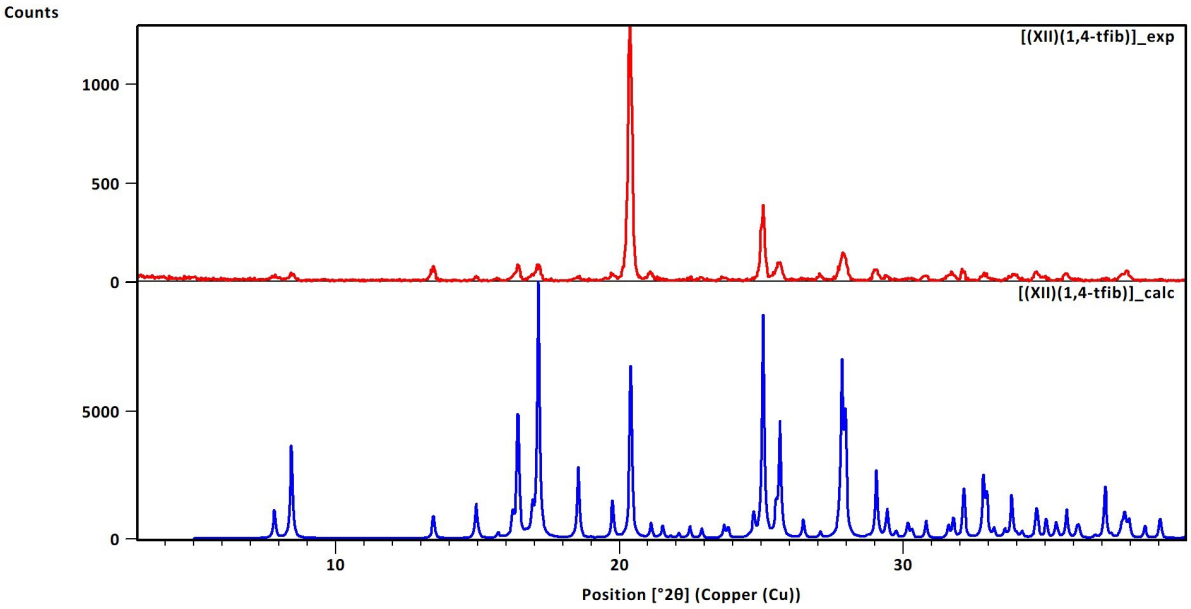

Figure 35. Experimental and calculated XRPD patterns of the (**XII**)(**1,4-tfib**).

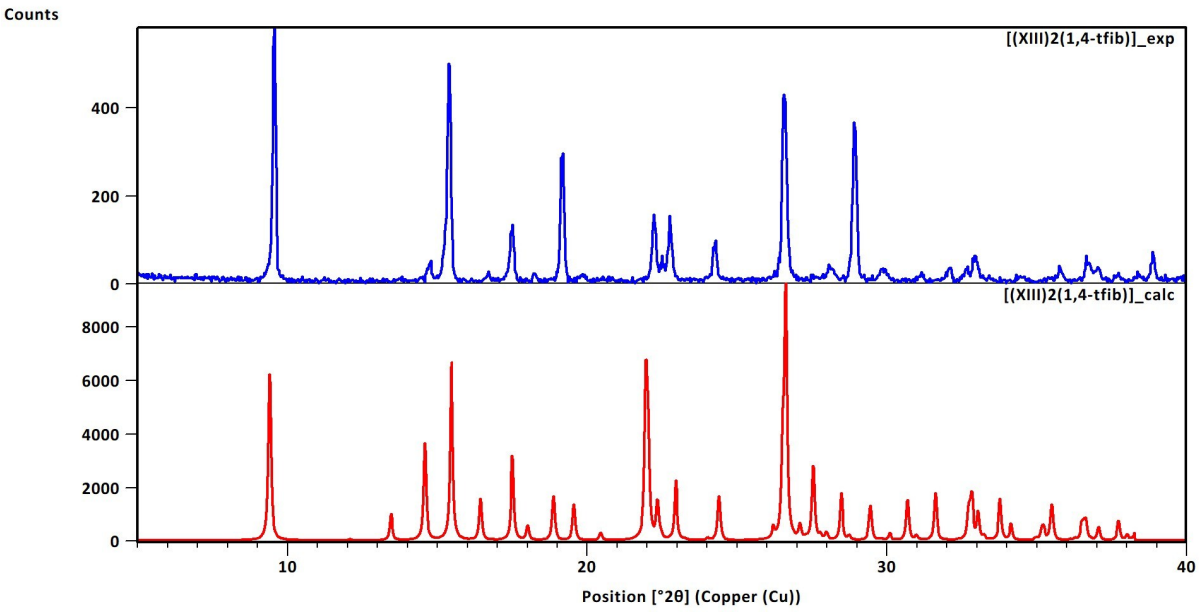

Figure 36. Experimental and calculated XRPD patterns of the (**XIII**)$_2$(**1,4-tfib**).

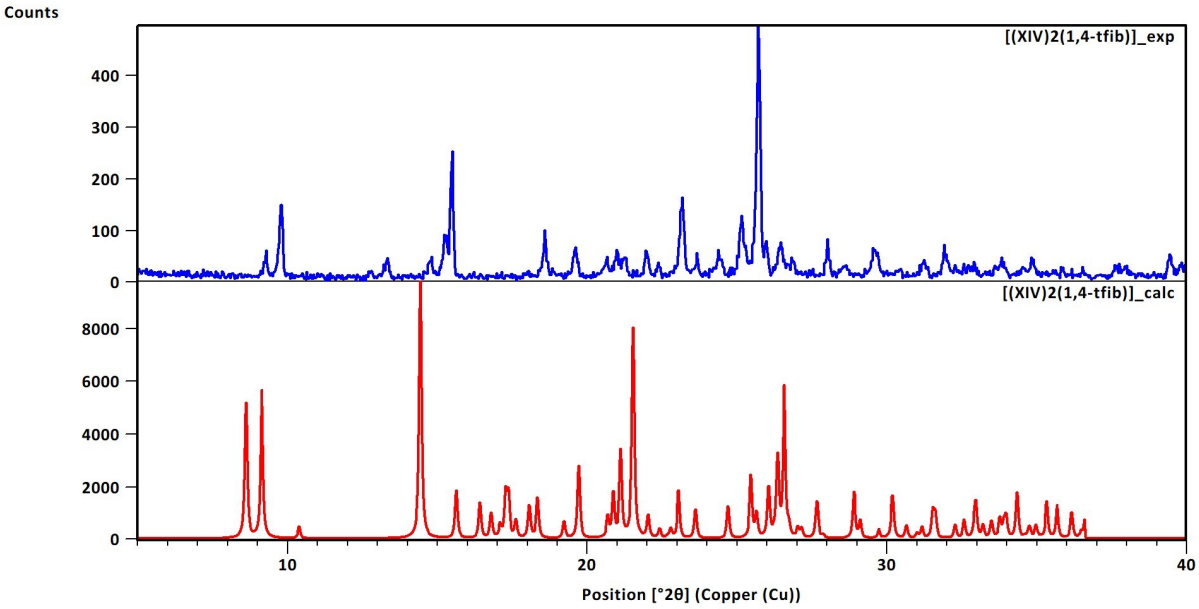

Figure 37. Experimental and calculated XRPD patterns of the (**XIV**)$_2$(**1,4-tfib**).

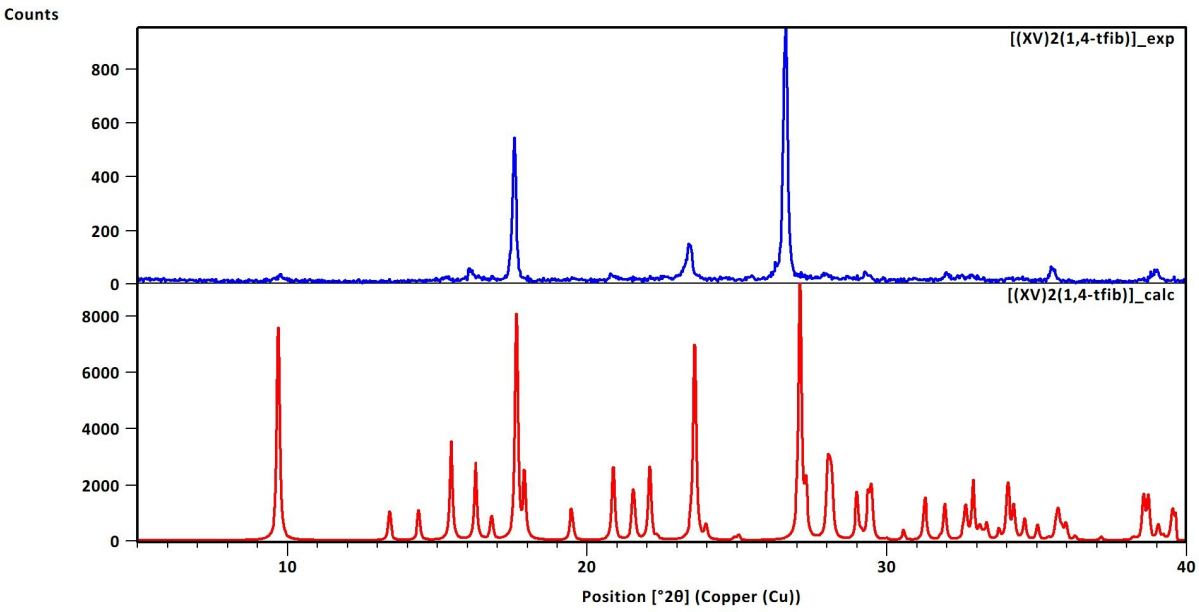

Figure 38. Experimental and calculated XRPD patterns of the (**XV**)$_2$(**1,4-tfib**).

Table 3. Melting/decomposition temperatures and corresponding molar enthalpies of the some prepared **1,3-tfib** cocrystals.

base	compound	ΔH / kJ mol^{-1}	T_e / °C
II	(**II**)(**1,3-tfib**)	−23.81	58.9
IV	(**IV**)(**1,3-tfib**)	−25.76	69.9
V	(**V**)(**1,3-tfib**)	−33.72	109.2
VI	(**VI**)$_2$(**VI**)(**1,3-tfib**)	−5.73	172.3
VIII	(**VIII**)(**1,3-tfib**)	−5.60	60.7
IX	(**IX**)(**1,3-tfib**)	−21.84	69.9
X	(**X**)(**1,3-tfib**)	−24.41	121.4
XI	(**XI**)(**1,3-tfib**)	−18.35	166.3
XII	(**XII**)(**1,3-tfib**)	−32.24	113.5
XIV	(**XIV**)(**1,3-tfib**)	−11.80	40.2
XV	(**XV**)(**1,3-tfib**)	−16.16	42.2
XVI	(**XVI**)$_2$(**1,3-tfib**)	−48.7	98.3

Table 4. Melting/decomposition temperatures and corresponding molar enthalpies of the some prepared **1,4-tfib** cocrystals.

base	compound	ΔH / kJ mol^{-1}	T_e / °C
I	(**I**)$_2$(**1,4-tfib**)	−34.86	88.1
II	(**II**)(**1,4-tfib**)	−12.33	50.2
III	(**III**)$_2$(**1,4-tfib**)	−34.75	99.6
IV	(**IV**)$_2$(**1,4-tfib**)	−49.06	109.1
V	(**V**)$_2$(**1,4-tfib**)	−57.43	153.4
IX	(**IX**)(**1,4-tfib**)	−31.46	127.4
X	(**X**)(**1,4-tfib**)		193.2
XII	(**XII**)(**1,4-tfib**)	−37.15	134.6
XIII	(**XIII**)$_2$(**1,4-tfib**)	−30.27	71.9
XIV	(**XIV**)$_2$(**1,4-tfib**)	−30.67	58.3
XV	(**XV**)$_2$(**1,4-tfib**)	−31.32	116.0
XVI	(**XVI**)$_2$(**1,4-tfib**)	−57.10	155.6

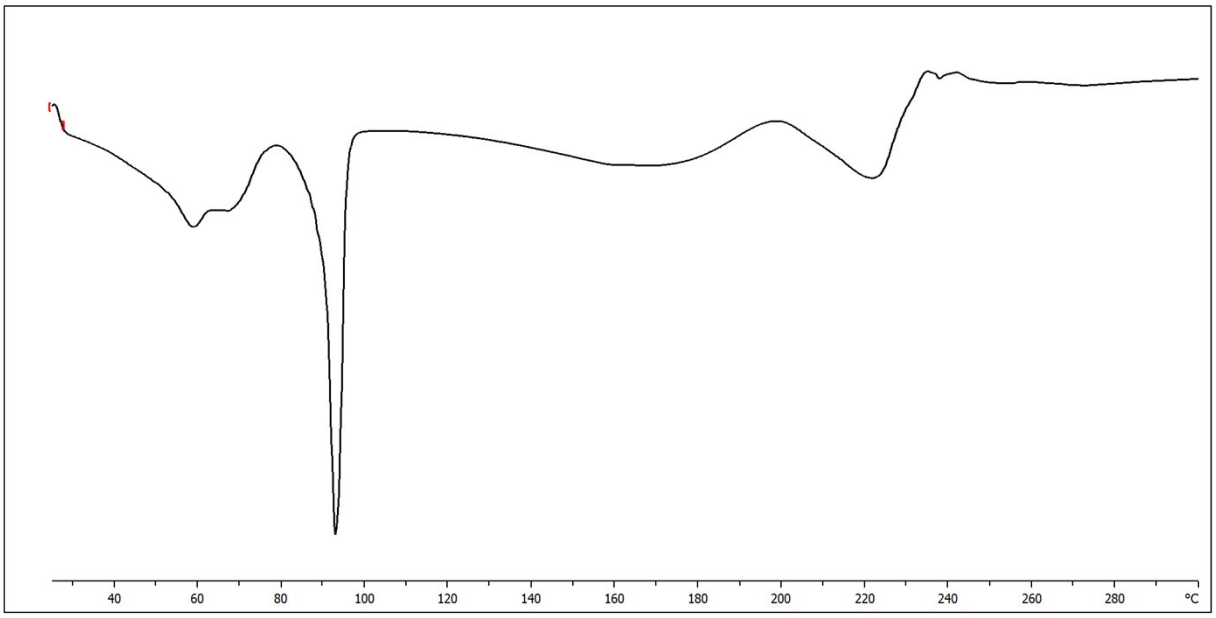

Figure 39. DSC curve of the (**I**)(**1,3-tfib**).

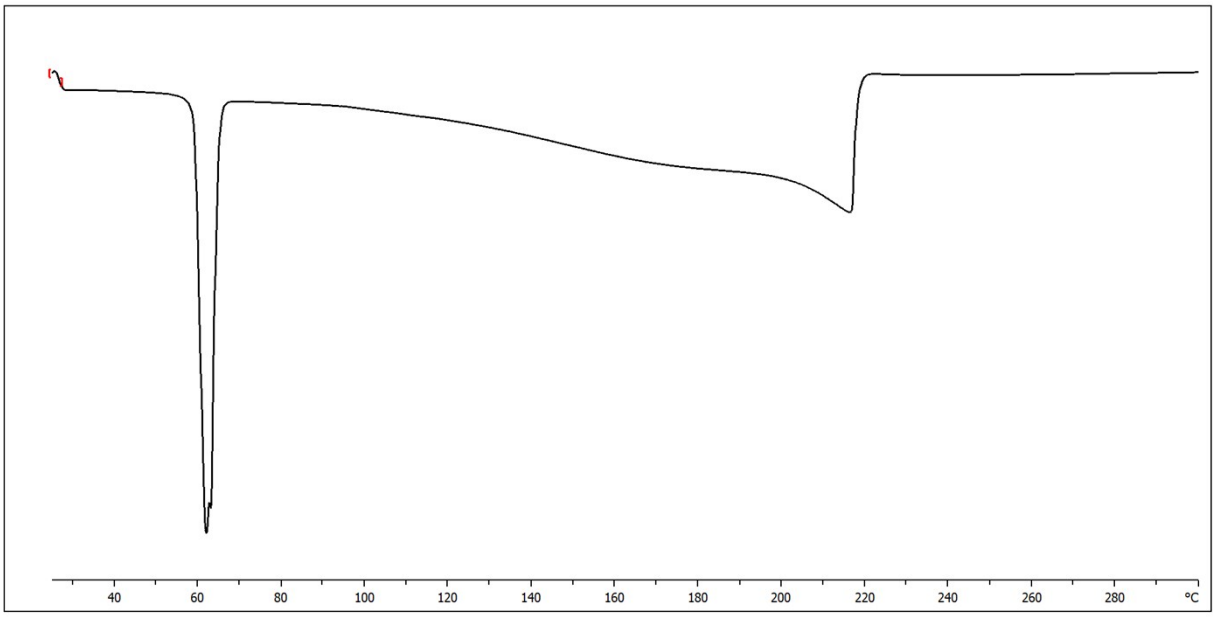

Figure 40. DSC curve of the (**II**)(**1,3-tfib**).

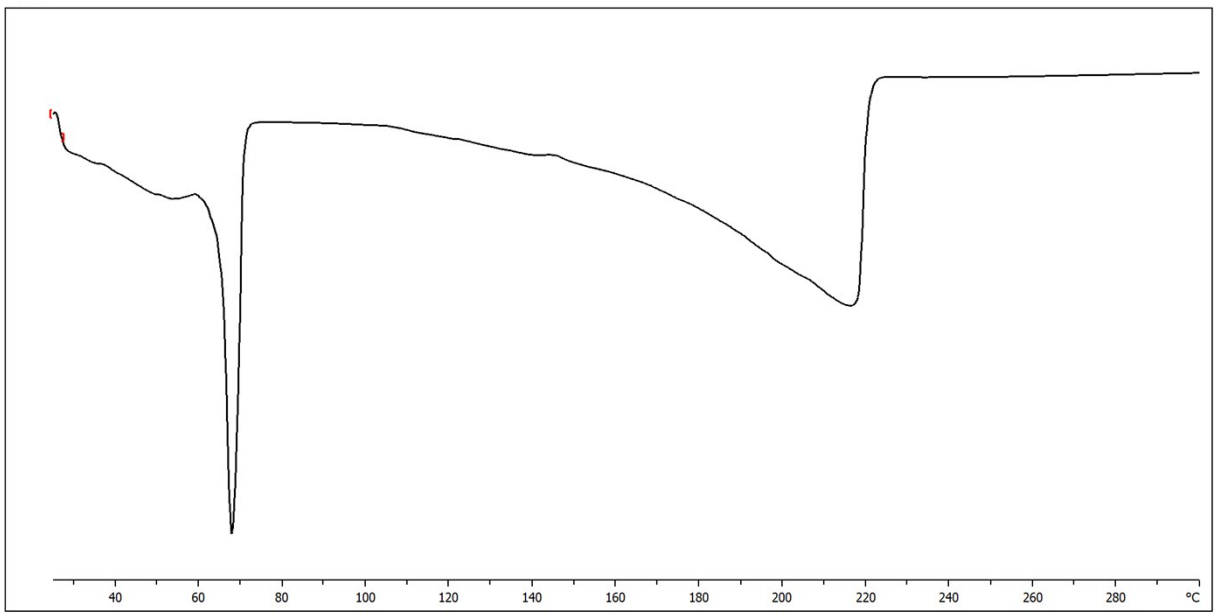

Figure 41. DSC curve of the (**III**)$_2$(**1,3-tfib**).

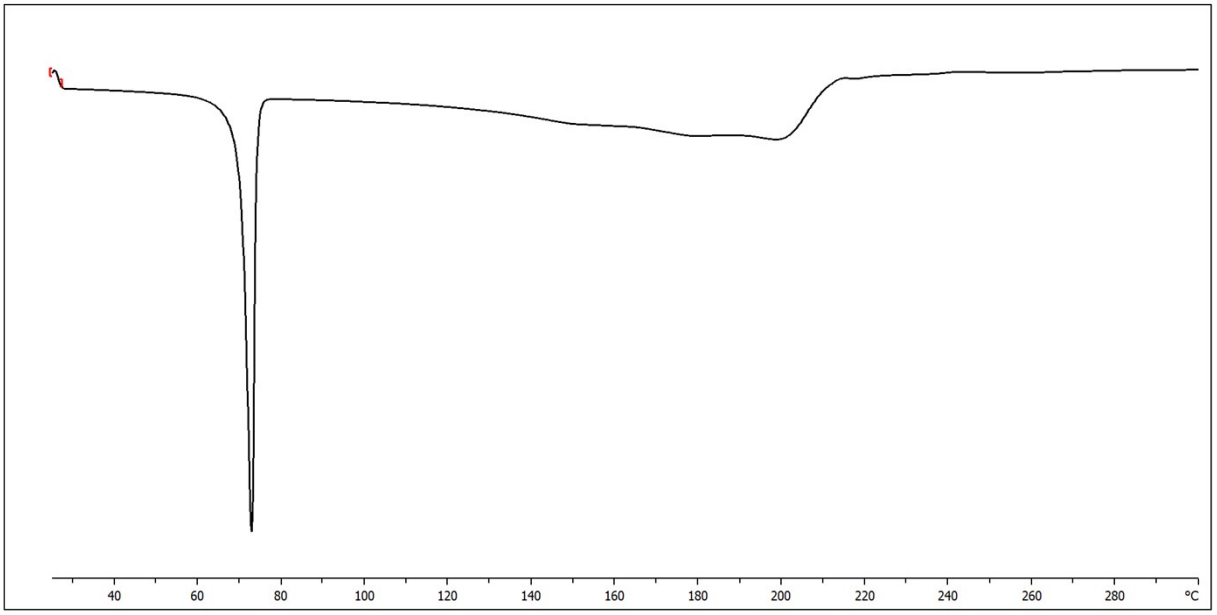

Figure 42. DSC curve of the (**IV**)(**1,3-tfib**).

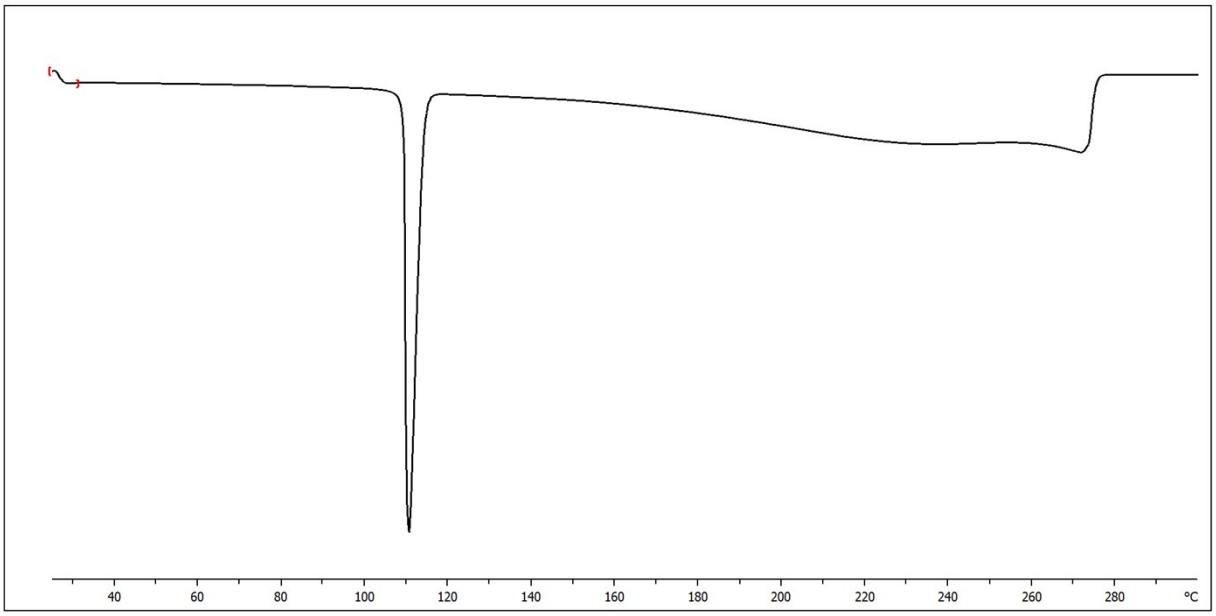

Figure 43. DSC curve of the (**V**)(**1,3-tfib**).

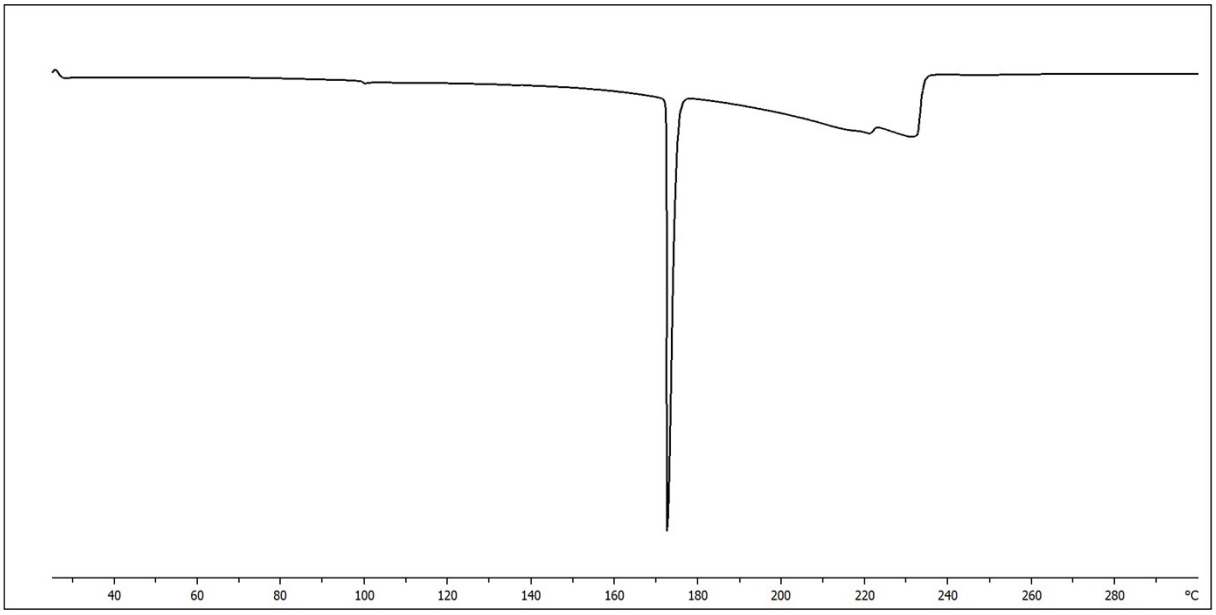

Figure 44. DSC curve of the $(\mathbf{VI})_2$(**VI**)(**1,3-tfib**).

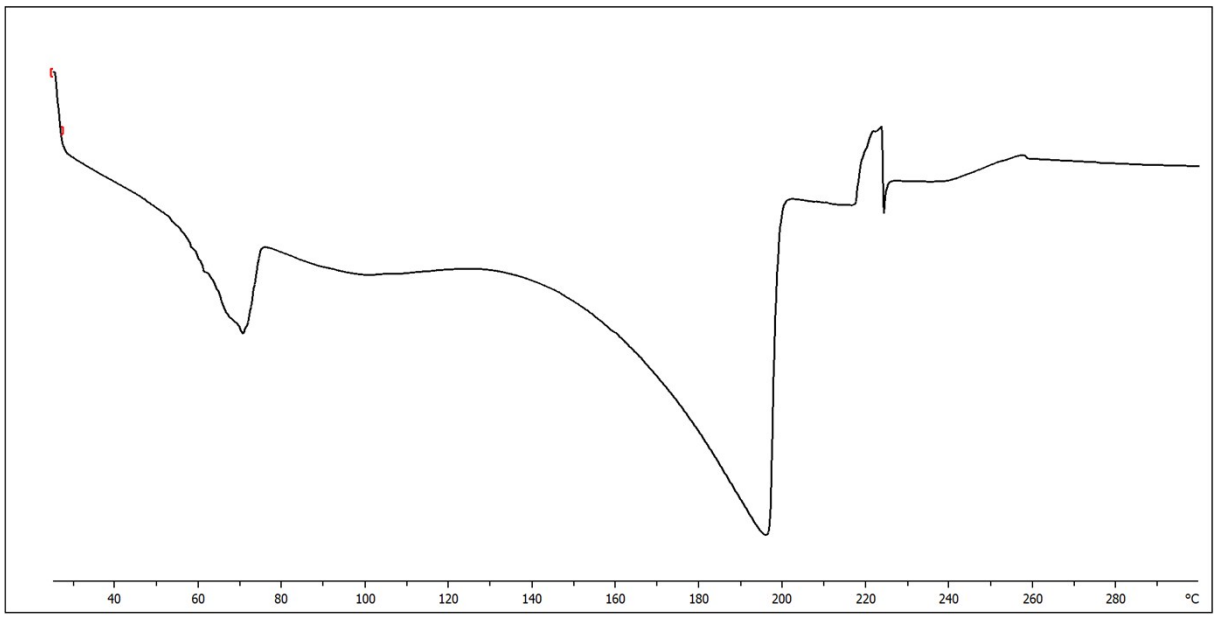

Figure 45. DSC curve of the (**VII**)(**1,3-tfib**).

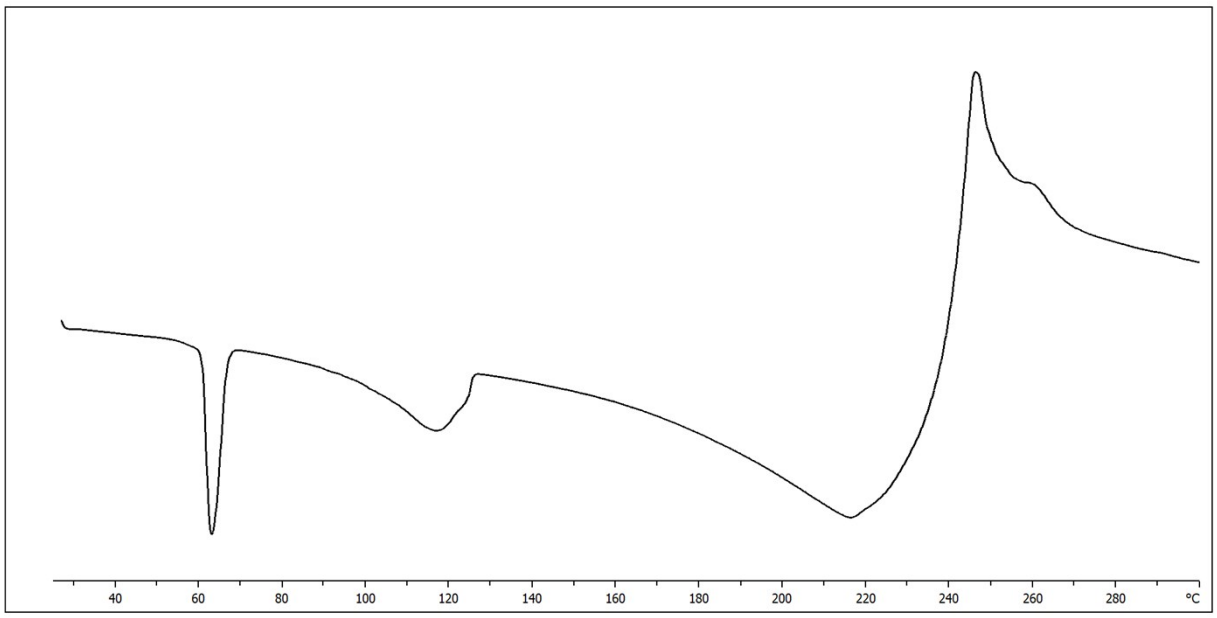

Figure 46. DSC curve of the (**VIII**)(**1,3-tfib**).

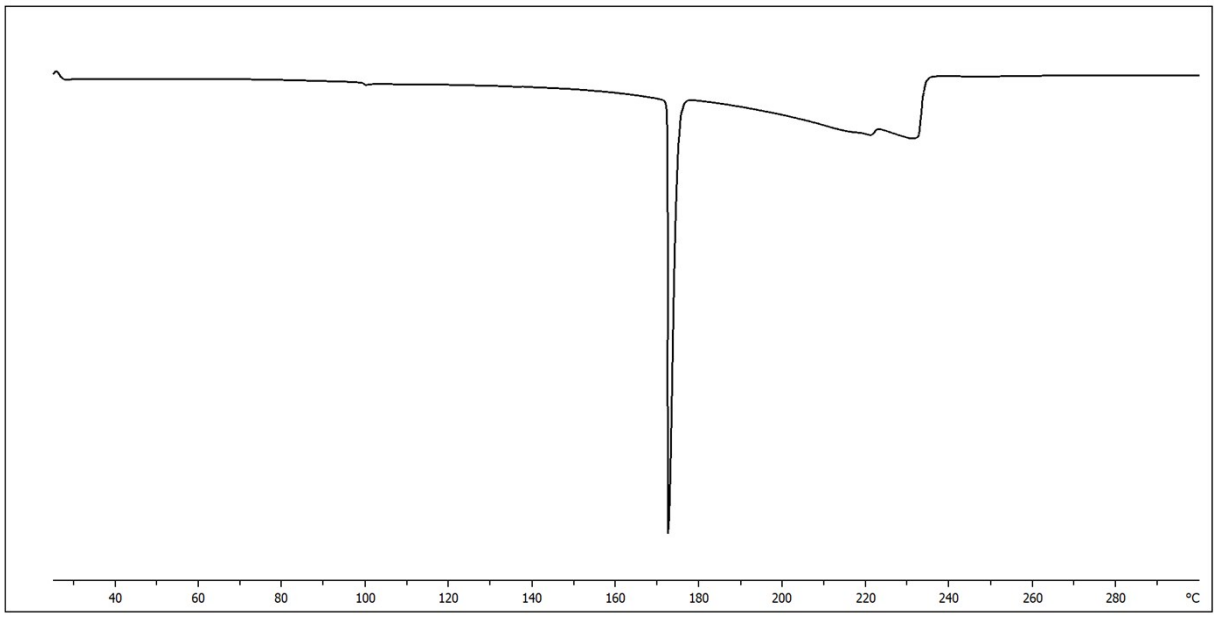

Figure 47. DSC curve of the (**IX**)(**1,3-tfib**).

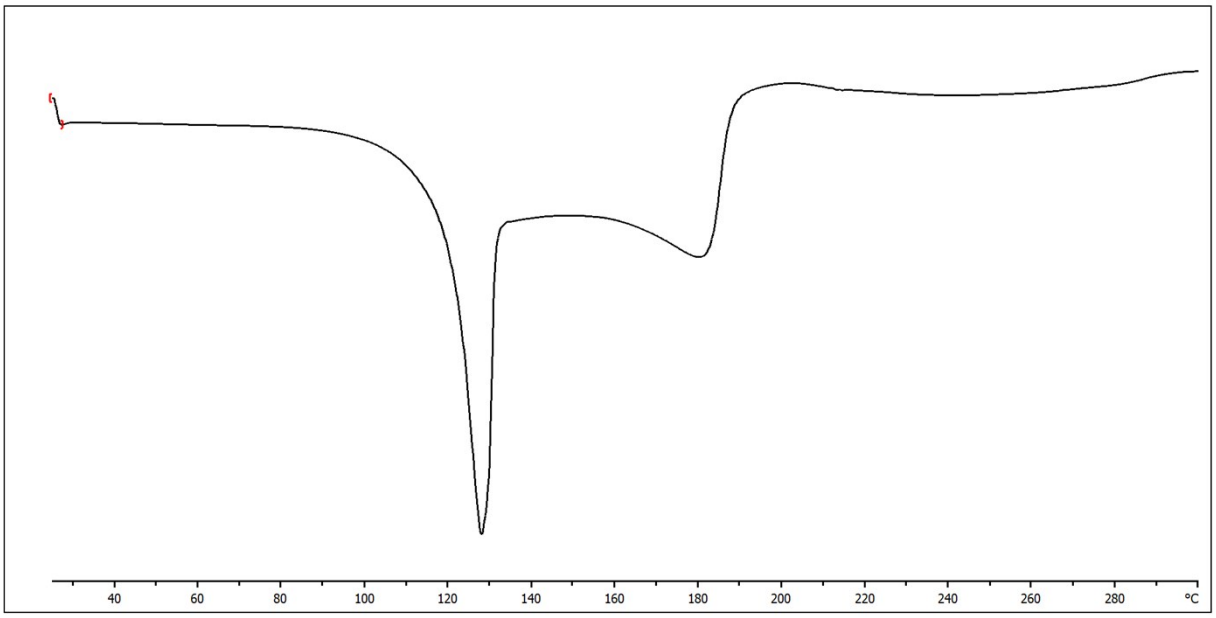

Figure 48. DSC curve of the (**X**)(**1,3-tfib**).

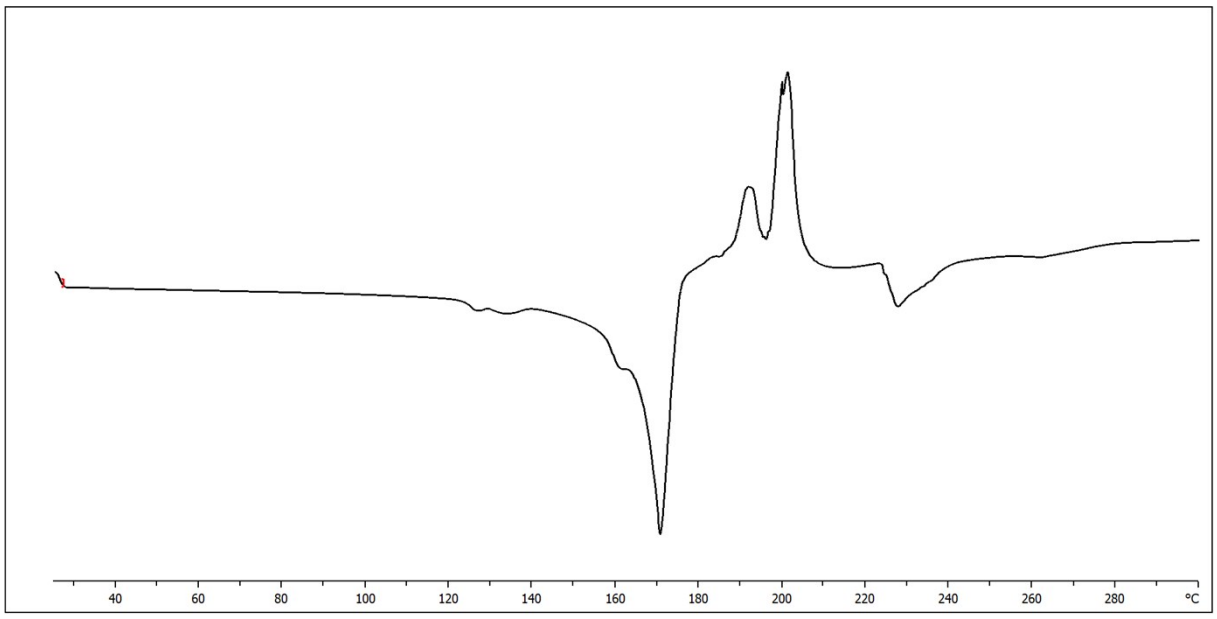

Figure 49. DSC curve of the (**XI**)(**1,3-tfib**).

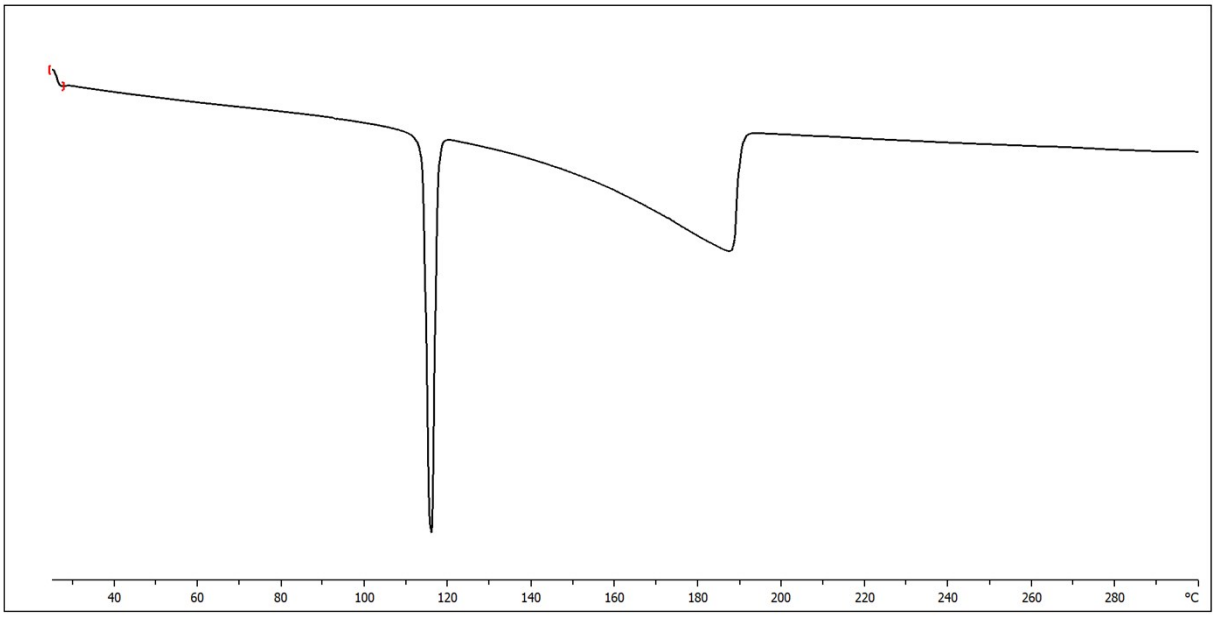

Figure 50. DSC curve of the (**XII**)(**1,3-tfib**).

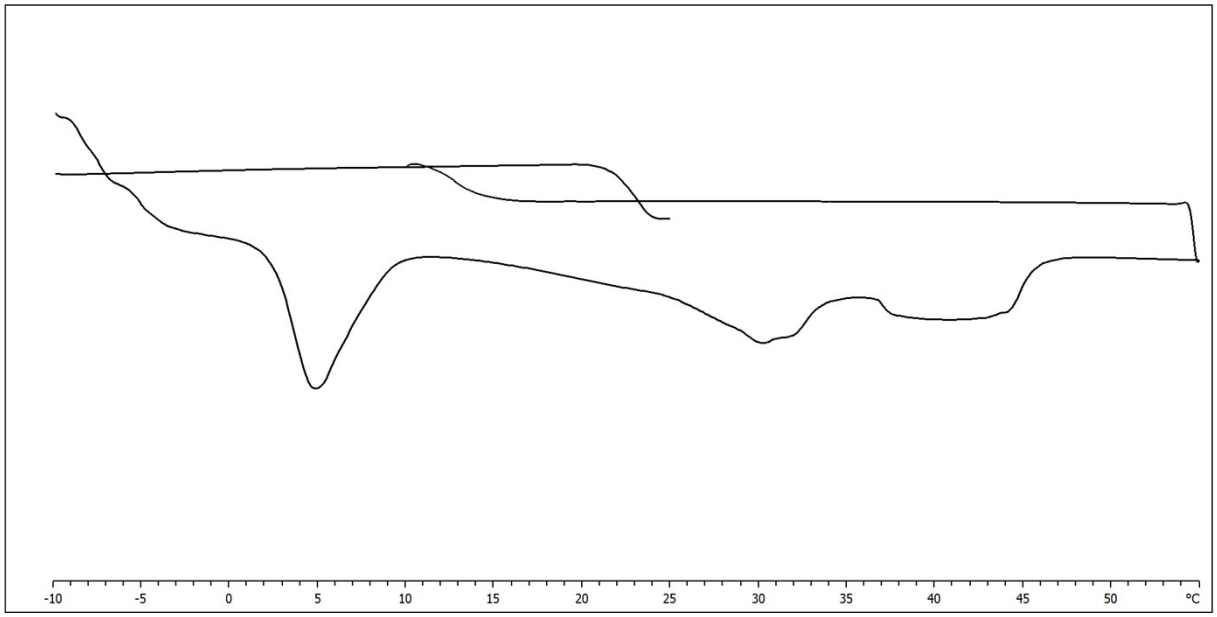

Figure 51. DSC curve for cooling and heating 1:1 mixture of the **XIII** and **1,3-tfib**.

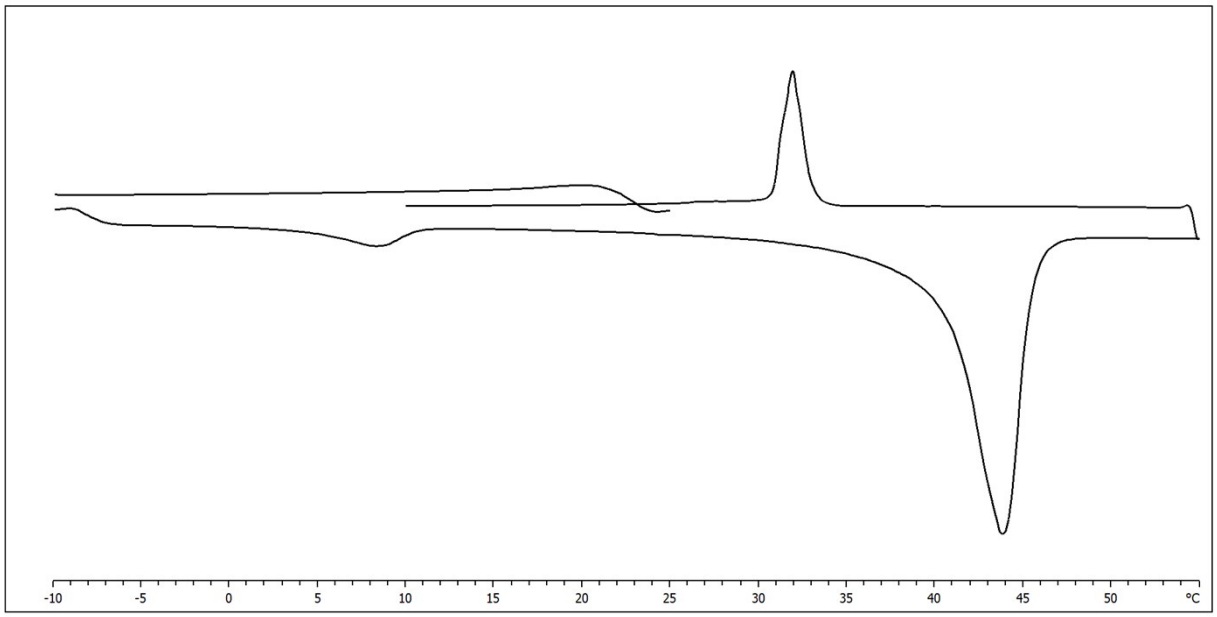

Figure 52. DSC curve for cooling and heating 1:1 mixture of the **XIV** and **1,3-tfib**.

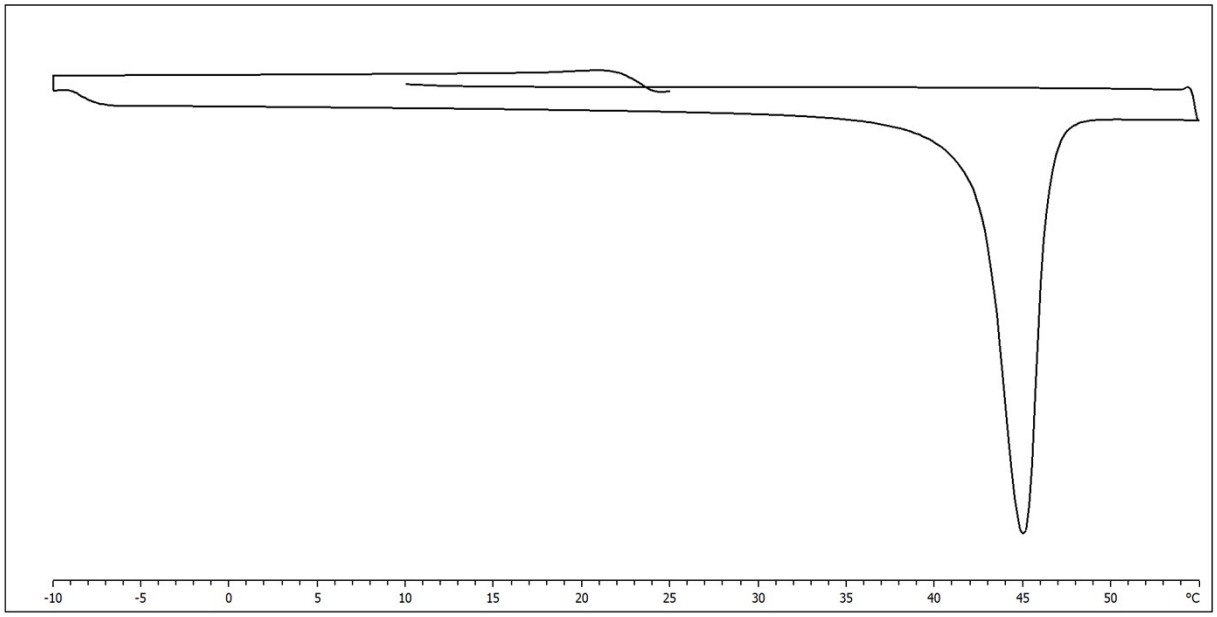

Figure 53. DSC curve for cooling and heating 1:1 mixture of the **XV** and **1,3-tfib**.

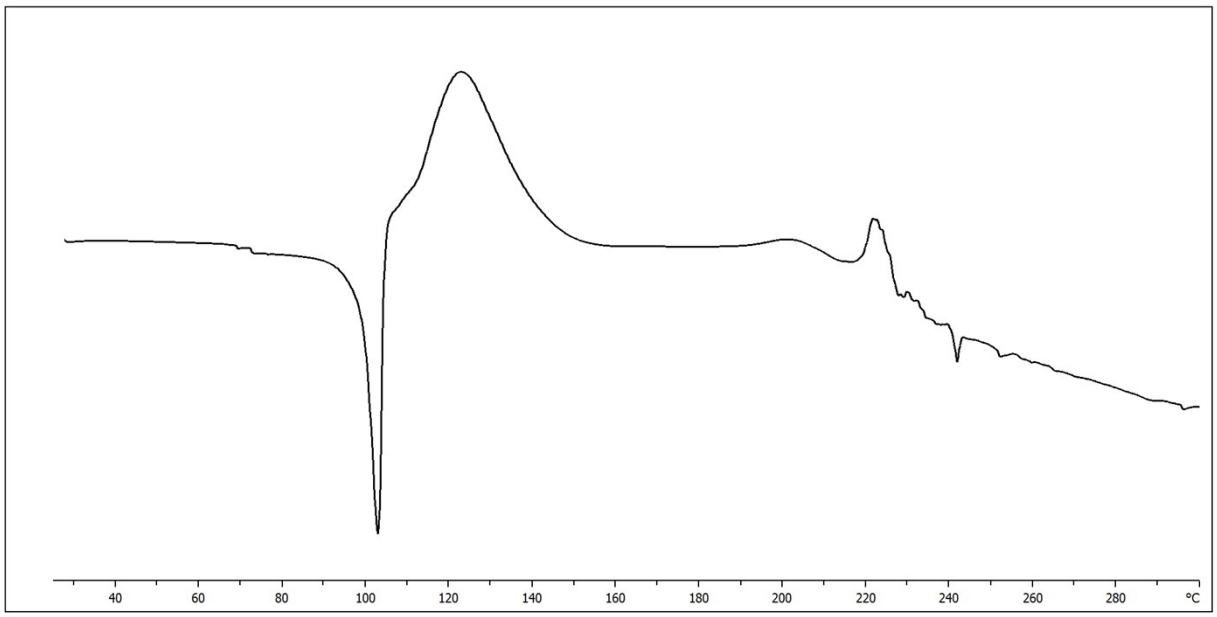

Figure 54. DSC curve of the (**XVI**)(**1,3-tfib**).

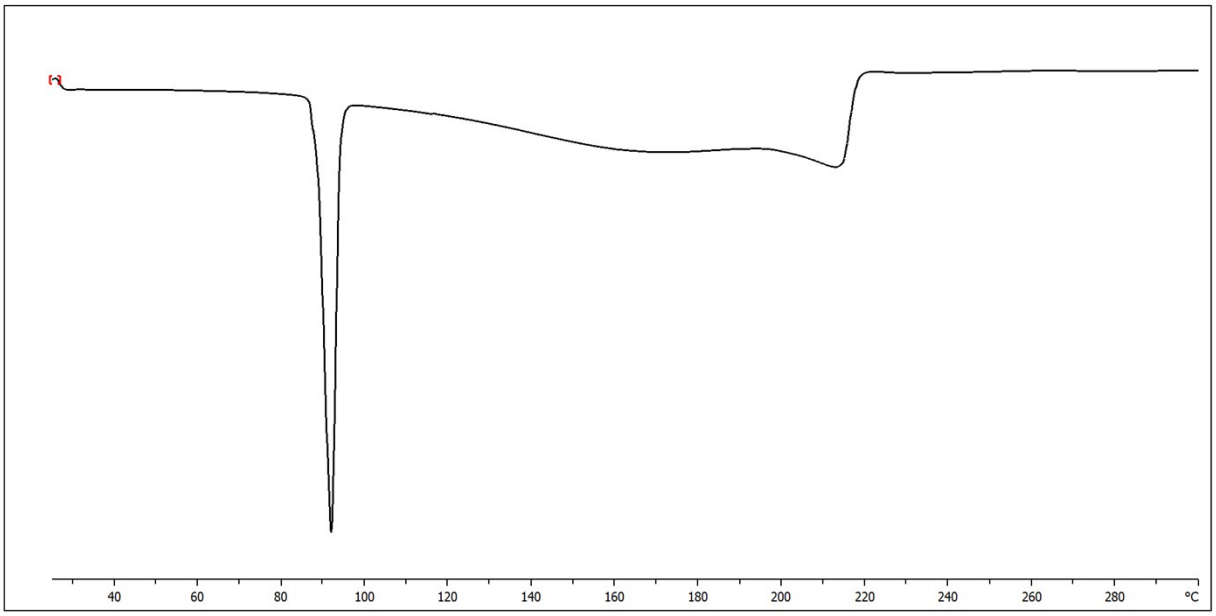

Figure 55. DSC curve of the (**I**)$_2$(**1,4-tfib**).

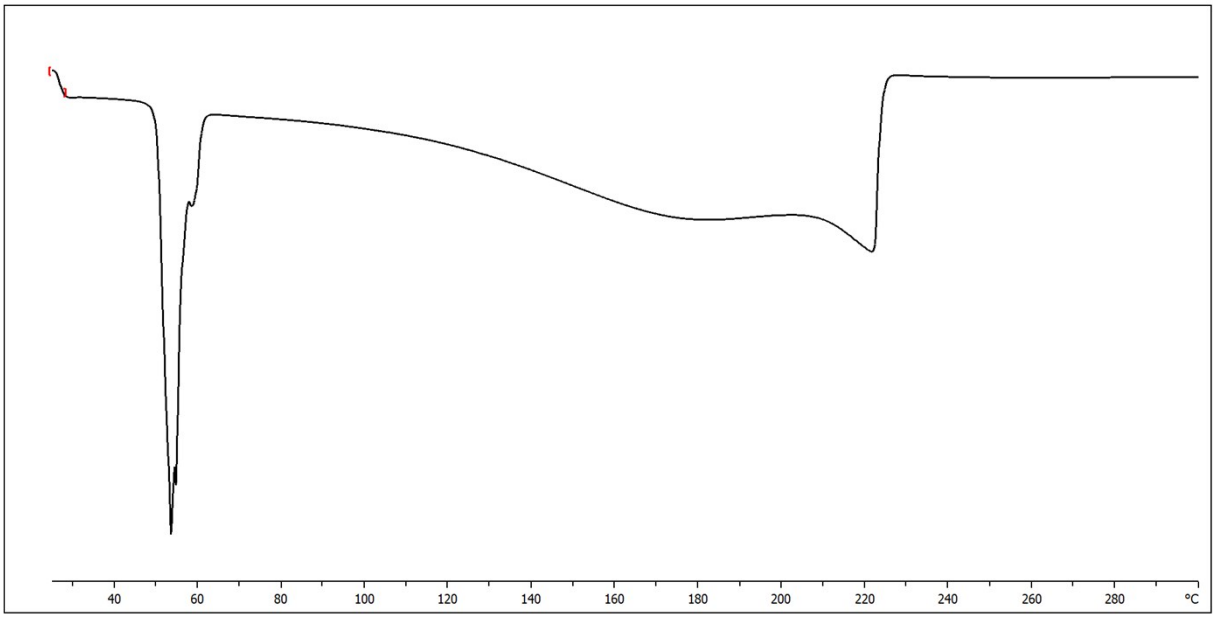

Figure 56. DSC curve of the (**II**)(**1,4-tfib**).

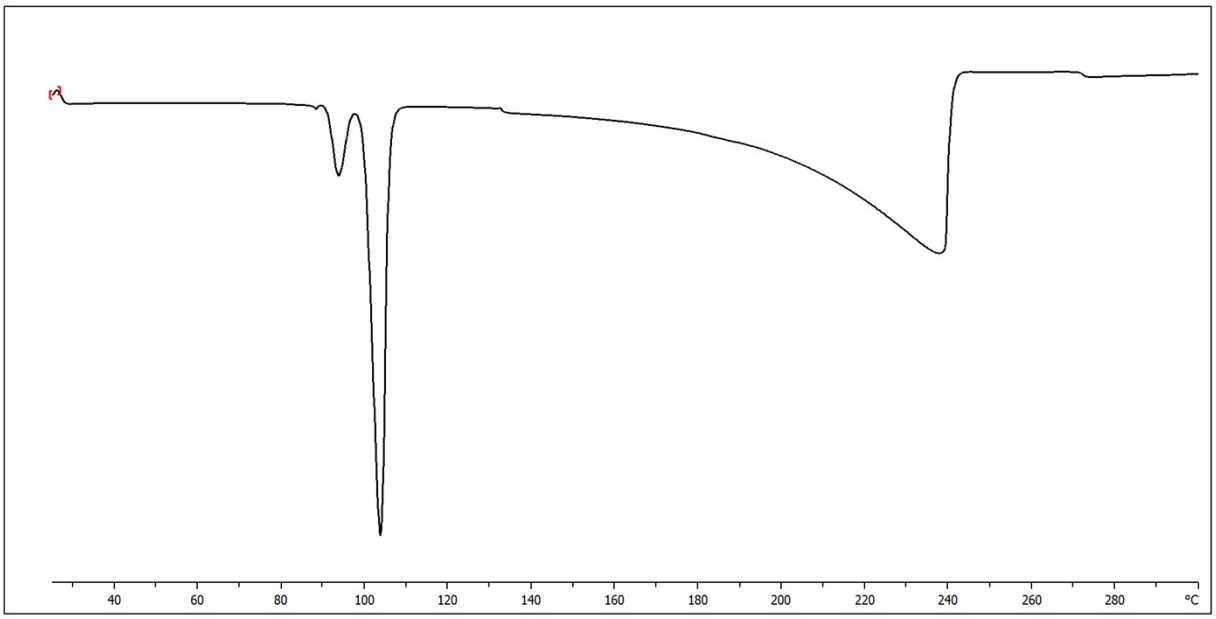

Figure 57. DSC curve of the (**III**)$_2$(**1,4-tfib**).

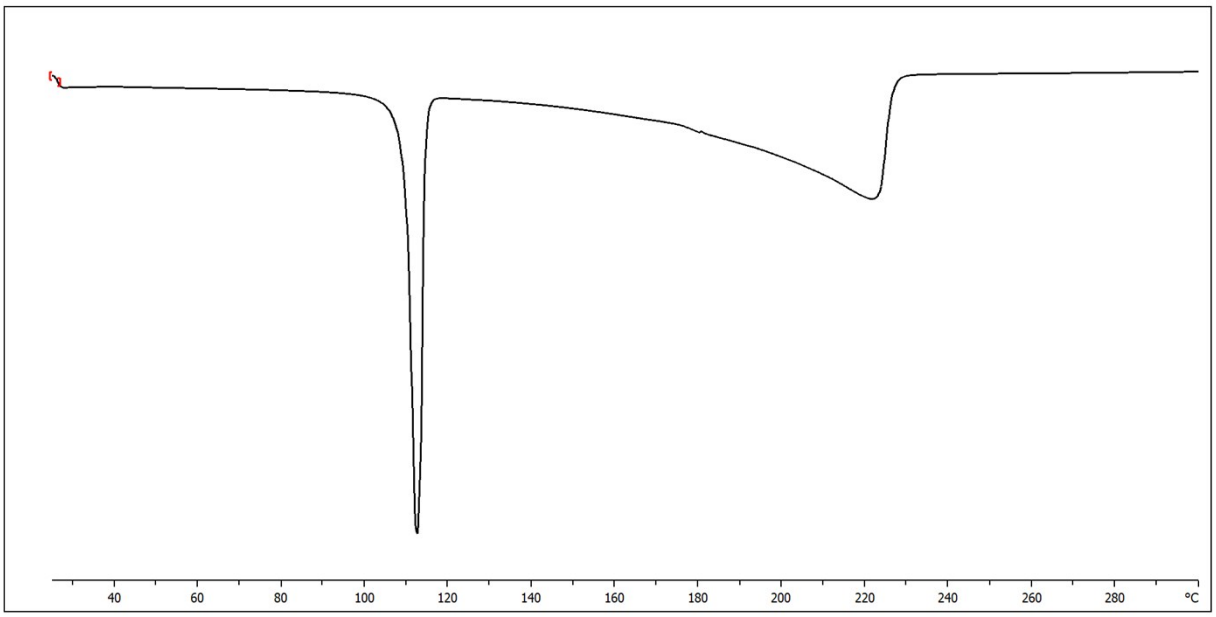

Figure 58. DSC curve of the (**IV**)$_2$(**1,4-tfib**).

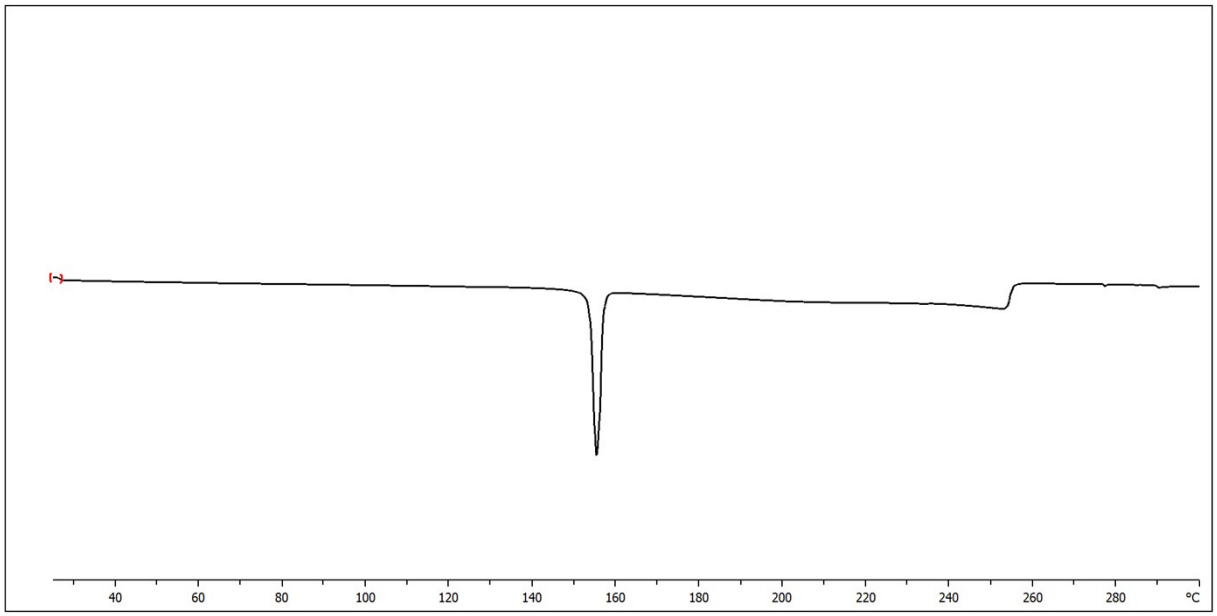

Figure 59. DSC curve of the (**V**)$_2$(**1,4-tfib**).

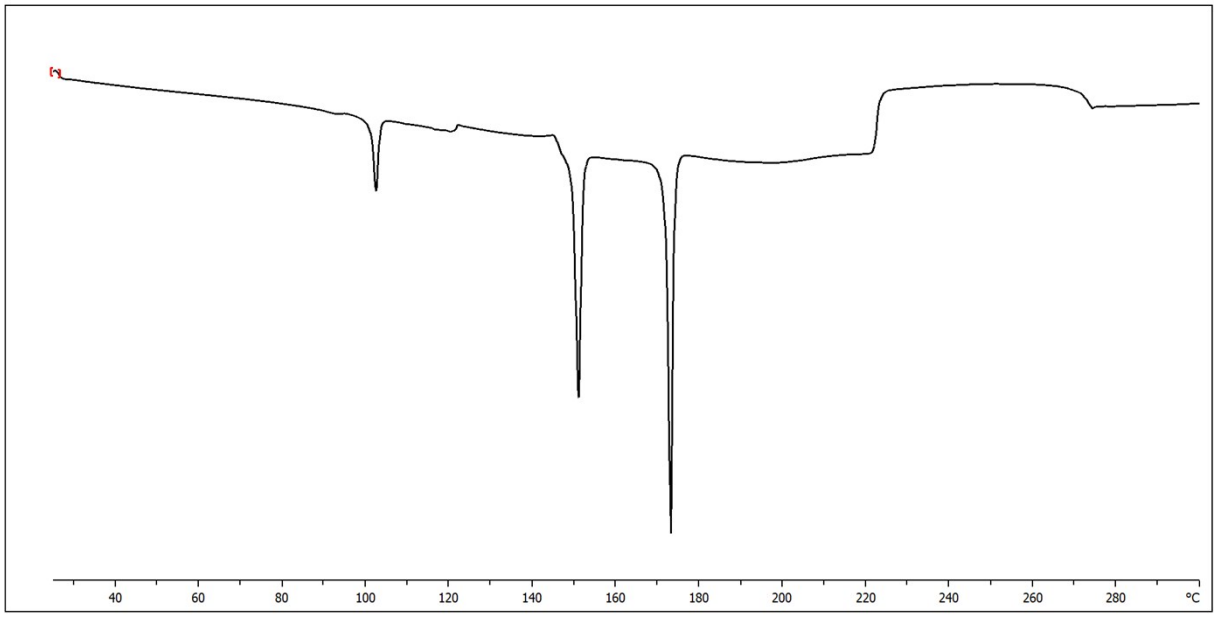

Figure 60. DSC curve of the (**VI**)$_2$(**1,4-tfib**).

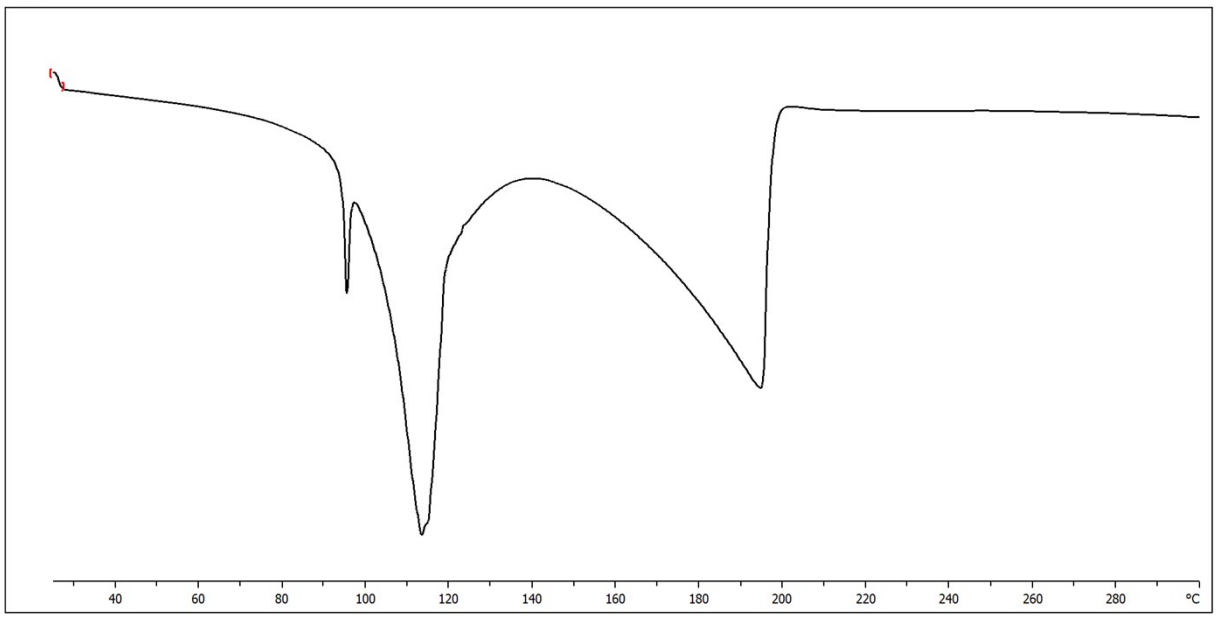

Figure 61. DSC curve of the (**VII**)(**1,4-tfib**).

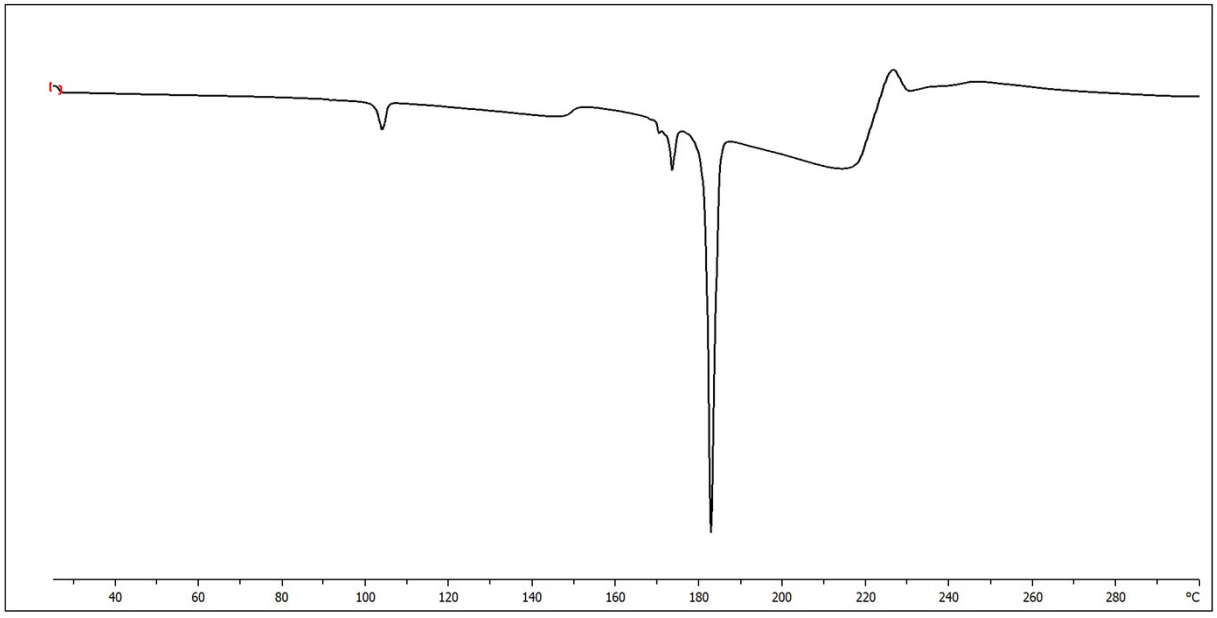

Figure 62. DSC curve of the (**VIII**)(**1,4-tfib**).

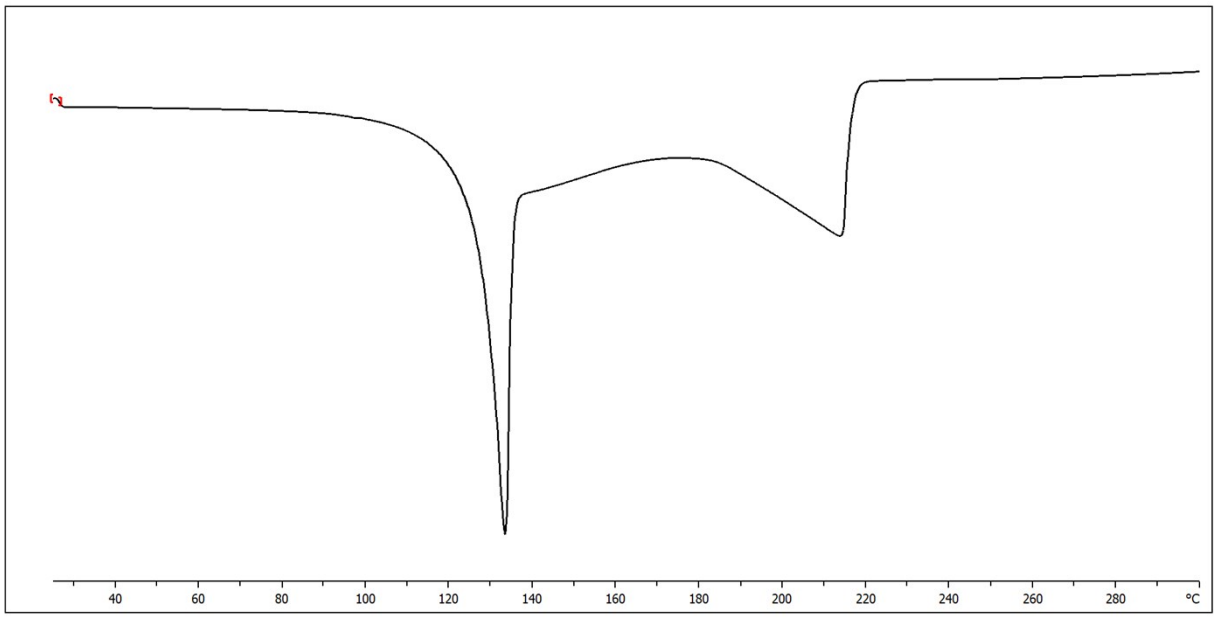

Figure 63. DSC curve of the (**IX**)(**1,4-tfib**).

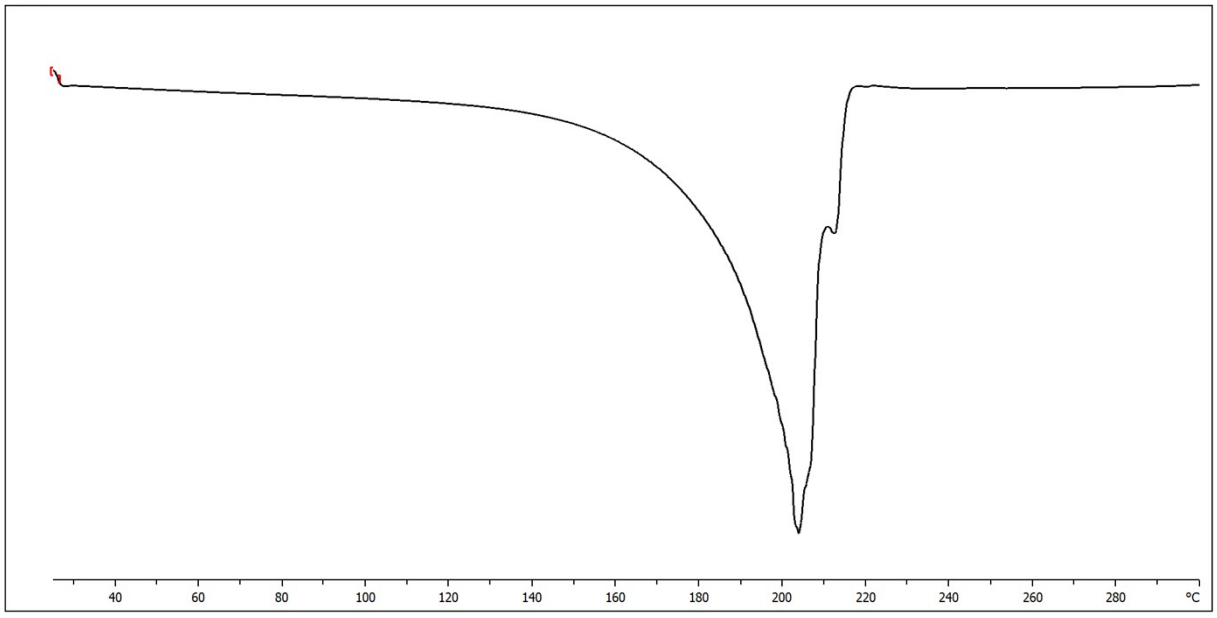

Figure 64. DSC curve of the (**X**)(**1,4-tfib**).

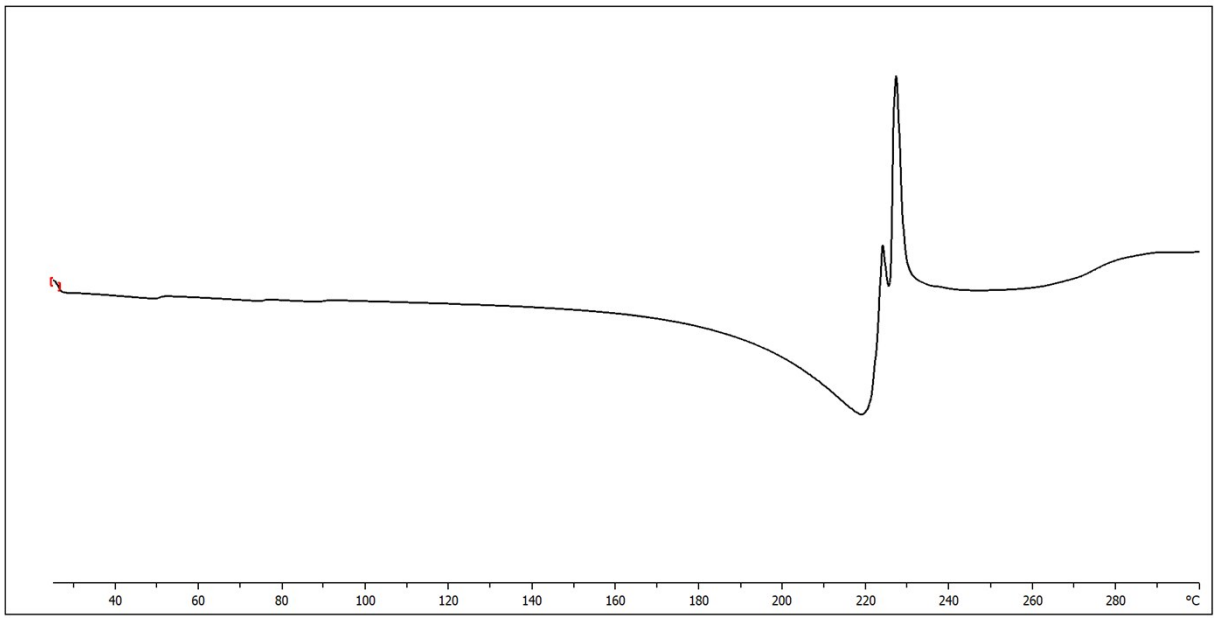

Figure 65. DSC curve of the (**XI**)(**1,4-tfib**).

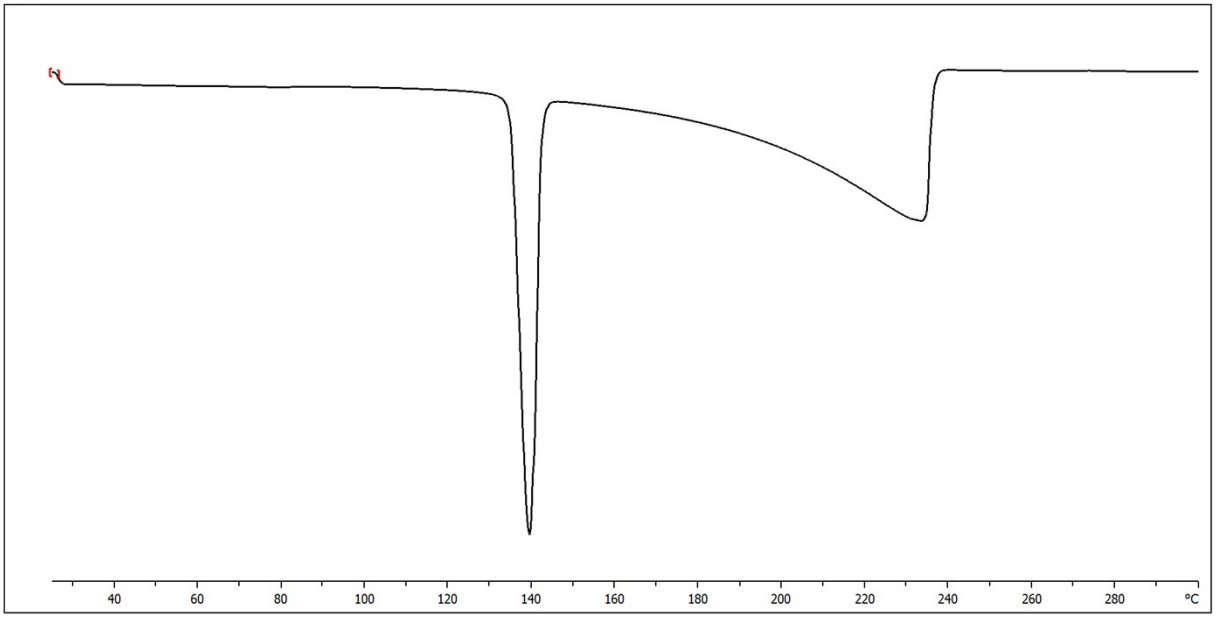

Figure 66. DSC curve of the (**XII**)(**1,4-tfib**).

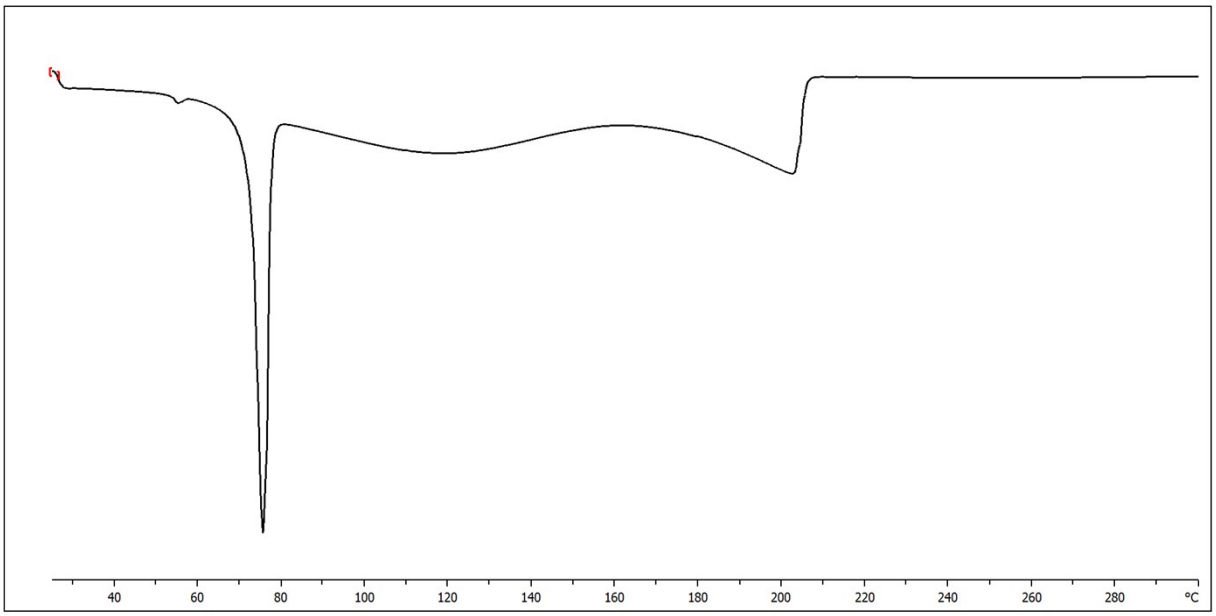

Figure 67. DSC curve of the (**XIII**)$_2$(**1,4-tfib**).

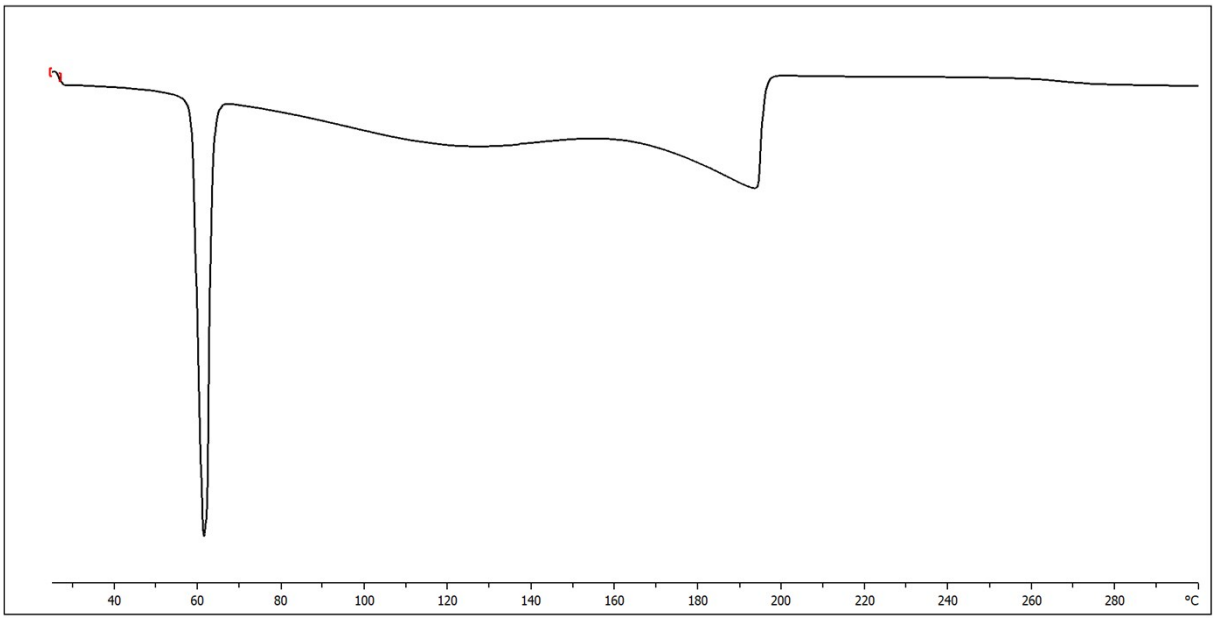

Figure 68. DSC curve of the (**XIV**)$_2$(**1,4-tfib**).

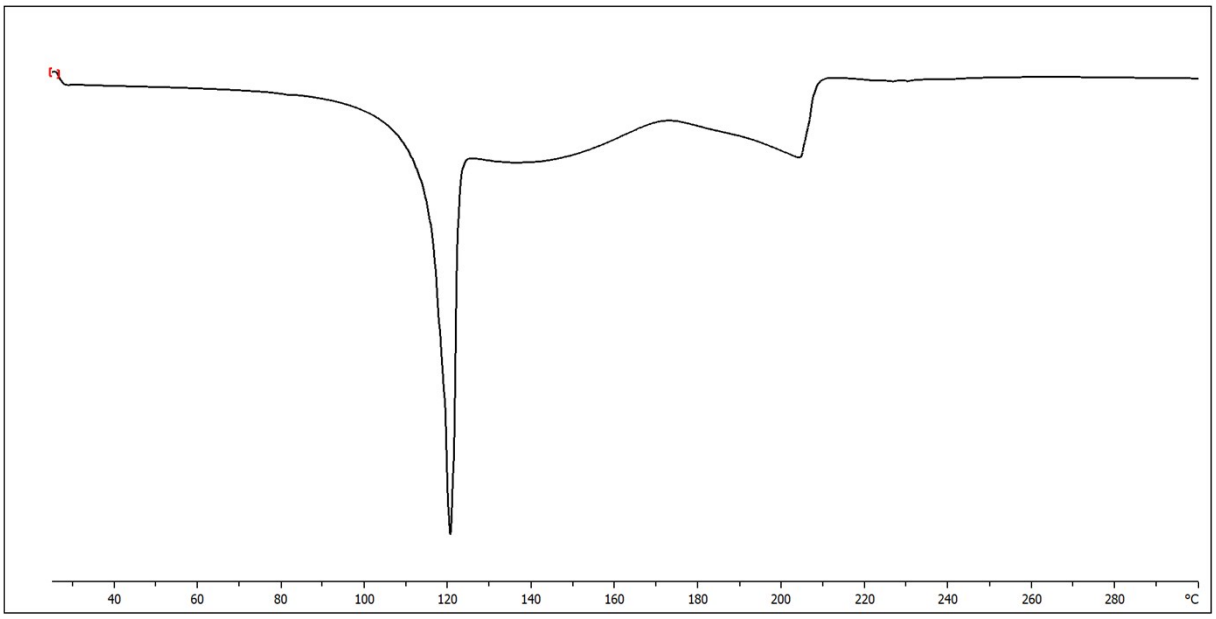

Figure 69. DSC curve of the (**XV**)$_2$(**1,4-tfib**).

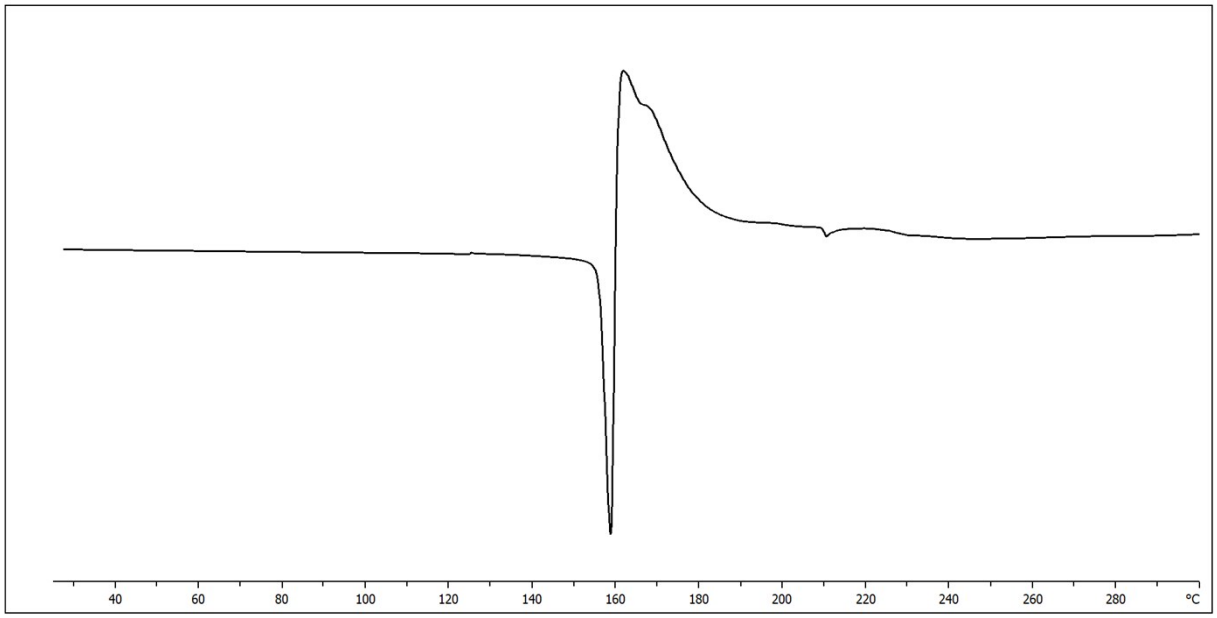

Figure 70. DSC curve of the (**XVI**)$_2$(**1,4-tfib**).